EARTHQUAKE ENGINEERING RESEACH INSTITUTE
2021 UNDERGRADUATE SEISMIC DESIGN COMPETITION

ARCHITECTURAL ENGINEERING SENIOR PROJECT FINAL REPORT

BY

TOMLINN COX

California Polytechnic State University

San Luis Obispo, California

Senior Project Advisor

Anahid Behrouzi, Ph.D.

2021

ACKNOWLEDGEMENTS

Special thanks to the 2021 EERI Cal Poly Student Chapter
for assisting in the production of work for the competition.

As well as our advisor Dr. Anahid Behrouzi, Civil Engineering Professor Dr. Babak Kamranimoghaddam, and Architectural Engineering Professors, Dr. Cole McDaniel, Dr. Radu Popescu, and Peter Laursen for their guidance and expertise.

ABSTRACT

Since 2004, the Earthquake Engineering Research Institute (EERI) has hosted the undergraduate Seismic Design Competition to promote the study of earthquake engineering. This year, a team of students from the California Polytechnic State University, San Luis Obispo competed against 36 other colleges and universities from across the world in the 19th annual competition, virtual for the first time due to the COVID-19 pandemic. The following report summarizes and expands on the material prepared by the 2021 team to guide the exploration of the implementation of an addition to an existing hospital that needs retrofitting. This includes the potential design sequence that could be implemented to complete such a project in the real world from research to analysis and design. Furthermore, this report highlights the depth of interdisciplinary subjects that this competition demands of participating teams and hopes to spark interest in other undergraduate students to participate in the competition.

TABLE OF CONTENTS

LIST OF FIGURES

LIST OF TABLES

SUPPLEMENTARY MATERIALS

The *Supplementary Materials* listed below were provided by the competition planning committee or generated as a solution by the 2021 California Polytechnic State University, San Luis Obispo Earthquake Engineering Research Institute (EERI) Seismic Design Competition (SDC) team. These documents are referenced throughout the body of this report to provide the reader with further context. All files listed below can be found in a zip folder submitted to Digital Commons @ Cal Poly as Supplemental Project files to this report.

1-1	2021 SDC Virtual Competition Outline
1-2	2021 SDC Scoring Document
4-1	Boring Log
4-2	P-S Suspension Log
4-3	Geotechnical and Seismicity Deliverable
4-4	Candidate Ground Motions
4-5	Design Response Spectrum, Python Code
4-6	PEER Ground Motion Database Time Series Search Report, NGA-West 2
4-7	Scaled Selected Seed Motions
5-1	Structural Deliverable
5-2	Existing Construction Documents
5-3	Scaled Time Histories
6-1	Structural Design Guide
6-2	Architectural and Environmental Deliverable
7-1	Retrofit Deliverable

1 COMPETITION DESCRIPTION AND OBJECTIVE

The 2021 Undergraduate Seismic Design Competition, hosted by the Earthquake Engineering Research Institute (EERI), was developed to promote the study of earthquake engineering among undergraduate students. This year's competition followed a completely virtual format, allowing the continuation of the competition during the COVID-19 pandemic. The competition was developed to ensure interdisciplinary work with four written deliverables involved. Research, design, and analysis were completed in the topic areas of: geotechnical engineering and seismicity, structural engineering, architecture and environmental impact, and seismic retrofitting. The competition also encourages students worldwide to begin building professional relationships with EERI to continue in engineering careers that focus on the design of seismically safe structures and communities.

See *Supplementary Material 1-1* for the competition format and *Supplementary Material 1-2* for the scoring document that further detail the outline and guidance from the EERI Student Leadership Council (SLC).

2 DESIGN PROMPT

The mayor of Seattle, WA is making a plea to acquire urgent funds to increase hospital space to keep up with the healthcare demand arising from the COVID-19 pandemic. Since there is a pressing need for space, an existing hospital structure in the Greater Seattle Area was chosen to expand with a proposed vertical extension that would increase patient capacity, with possibility of a seismic retrofit based on a performance assessment.

3 APPLICABLE CODES

The following list outlines the code provisions that were generally used to complete the respective deliverable topics:

- ASCE 7-16 Provisions, Minimum Loads and Associated Criteria for Buildings and Other Structures [1]
- ASCE 41-17, Seismic Evaluation and Retrofit of Existing Buildings [2]
- NDS Supplement 2018, National Design Specifications, Design Values for Wood Construction [3]

4 EXISTING SITE CONDITIONS

4.1 SOIL CONDITIONS

To assess the soil conditions at the proposed site (47.6163, -122.3534), a Boring Log and P-S Suspension Log were provided, refer to *Supplementary Materials 4-1* and *4-2* respectively. This information, along with outside research, allowed students to develop an understanding of geotechnical engineering reports conducted before the design of a structure.

4.1.1 General Subsurface Conditions From Boring Log

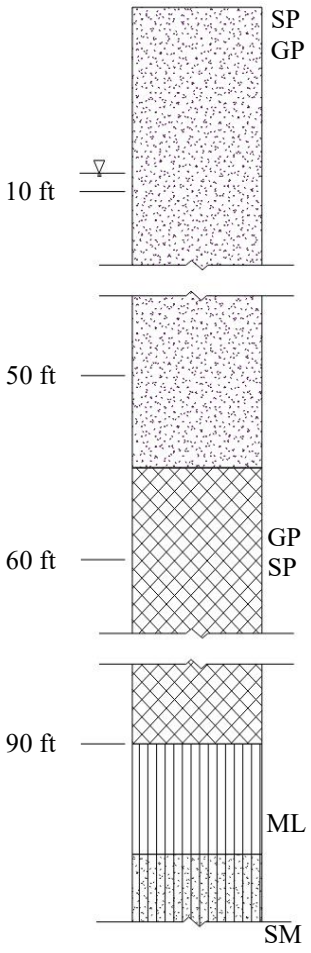

Figure 4.1:
Modified Boring Log

The modified site Boring Log, represented in **Figure 4.1**, presents an undesirably high ground water table at a depth of 9.5 ft, such that all the soil below this point is saturated. This is of concern because it could affect the stability of the foundation system, as it alters the pore water pressure and thus the stress of the soil. In addition to the high ground water table, the soil types at the site pose a great risk for liquefaction, a process in which the soil behaves as a liquid in a seismic event, impacting building integrity.

There are two zones with the most risk for liquefaction at the site. The first occurs 10 ft to 40 ft beneath the surface. At this depth, the fill soil is noted as being loose to medium dense, saturated very gravelly sand to very sandy gravel with silt. Most liquefaction hazards are associated with sandy and silty soils of low plasticity, as cohesive soils are generally not considered susceptible to this condition [4]. The site having poorly graded sandy and gravelly soil, designated as SP and GP in **Figure 4.1** respectively, both with little to no cohesion, poses danger. The Standard Penetration Resistance (N-SPT) was provided as part of the Boring Log and informs of blows per foot reporting as low as four in this region at 15 ft. Based on this low N-SPT and inherent liquefaction of the loose saturated sand, this zone will have the highest likelihood of liquefaction. Furthermore, this region is of concern due to the particle sizes that are attributed to the soil types. Coarse-grained (gravels and sands), saturated (high moisture content) soils are very susceptible to liquefaction because they tend to densify when shaken in seismic events, leading to a tendency of pore volume reduction and subsequent increase in pore water pressure [5,6]. Increased pore water pressure results in a corresponding reduction of the effective stress and therefore reduced shear strength. The soil begins to behave

increasingly like a liquid as it undergoes shaking, leading to a complete loss in shear strength when the effective stress is reduced to zero.

Another area of concern consists of the very soft, wet silt layer and the loose silty sand layer at depths between 90 ft to 98 ft, where a shift in make-up can be seen in **Figure 4.1**. These soil types are noted as ML from 90 ft to 96 ft for the inorganic silts and SM from 96 ft to 98.5 ft for silty sand. The silt layer is at risk for liquefaction due to its low plasticity and moisture content of approximately 90% of the liquid limit, a state in which the water content of the soil changes from a plastic to a liquid state [6]. The silty sand layer is at risk due to the inherent liquefaction likelihood of loose, wet, sand as previously discussed. However, it is possible that these are not continuous layers and due to the depth, it is less likely that these layers will induce large lateral ground deformations in a seismic event, so they may not have a significant effect on the above hospital structure. If there are additional borings in the vicinity that could prove these layers to be continuous or not, they should be included in this study.

Due to the highly liquifiable soils from 10 ft to 40 ft, piles should be driven well into the medium dense sand layer to a depth of about 60 ft below grade. This would ensure that the deep foundation is supported by a competent soil layer. However, if the soil above liquifies, the piles may be sheared regardless of the firm anchoring in the competent medium dense gravel.

4.1.2 Ground Improvement Techniques

To mitigate the potential effects of liquefaction that were seen through analysis of the Boring Log, vibro-compaction on the surface from 10 ft to 40 ft and grouting from 90 ft to 98 ft were selected from a variety of ground improvement options. Vibro-compaction is a process that densifies loose sand fill to create stable soil by vibrating and saturating the soil grains while simultaneously adding clean sand or gravel [7]. This technique is particularly applicable to the upper layer of sandy gravel fill because it will compact the soil and in turn increase the strength, allowing for a more stable foundation and reduced risk of liquefaction. While this method could apply to the deeper soil type in discussion, the instrument is not designed to compact soil at depths greater than around 80 ft. Instead, the design team opted to apply a grouting technique that injects material into the soil to change the physical characteristics of the deeper soil layer [7]. By modifying the soil type and increasing the strength with applied properties, the soil will be altered in strength and drainage, leading to improved behavior of the soil and the foundation design. The different soil types require specific ground improvement techniques to reduce the risk of potential liquefaction.

4.1.3 ASCE 7-16 Site Class

If it were assumed that no ground improvement techniques were conducted at the site, it was determined that the site falls under Site Class F because the soil layers identified in **Section 4.1.1** are susceptible to liquefaction. This is due to the criteria listed in Section 20.3.1 of ASCE

7-16 [1] in which “soil is vulnerable to potential failure or collapse under seismic loading, such as liquefiable soils”. However, with this selection it is necessary to perform further soil analysis.

If the liquefaction mitigation per **Section 4.1.2** is performed, assuming the in-situ shear wave velocity is unaffected, the calculation of shear wave velocity for the top 100 ft of soil becomes necessary to classify the soil. In *Supplementary Material 4-2*, a P-S Suspension Log was provided by Global Geophysics that provided both P-wave velocity, as well as S-wave velocity values from 7.9 ft to 164 ft below the surface of the soil. Per ASCE 7-16 Section 20.4.1 [1], the shear wave velocity, $V_{S,30}$ was calculated to be 573 ft/s, see **Appendix 4.1.3** for calculations. Entering ASCE 7-16 Table 20.3-1 [1] with this value, Site Class E (soft clay soil with a $V_{S,30}$ less than 600 ft/s) was determined for the site. The shear wave velocity being unaffected by liquefaction mitigation is unusually conservative, so a more realistic site class would be D. Further analysis on the structure will continue with the more realistic choice of Site Class D, to account for applied mitigation techniques and modified soil parameters.

4.2 EARTHQUAKE HAZARD

To determine the seismicity of the region and properly assess it for seismic hazards, research must be conducted at the proposed site (47.6163, -122.3534). With this knowledge, a design response spectrum can be generated, in which known ground motions can be scaled to best replicate the potential seismic shaking of the site.

4.2.1 Fault Mapping of Site

The site in the Belltown Neighborhood of Seattle lies several blocks from the waterfront at Elliot Bay, placing the existing structure in an area of high seismic activity. As shown in **Figure 4.2**, the site (indicated by the star marker) is situated at an intersection between the Pacific Plate, Juan de Fuca, and the North American Plate, where there is risk of the Juan de Fuca Plate subducting under the North American Plate in an area known as the Cascadia Subduction Zone (CSZ) [8]. Earthquakes in the CSZ are responsible for deeper, longer, and higher magnitude events, inducing a resonance response in taller buildings. In addition to the subduction interface, the area of Seattle around the site is subject to smaller thrust faults. The nearby faults of greatest concern are within the Seattle Fault Zone that runs East-West through the city with an earthquake magnitude potential of 7.5 [9]. Thrust faults within this zone are near the crust’s surface where a rupture would cause intense shaking near the epicenter that would diminish with distance. This type of fault is of concern to structures because the aggressive, short duration of shaking causes a harsh jolt in the structure, resulting in a large impact force.

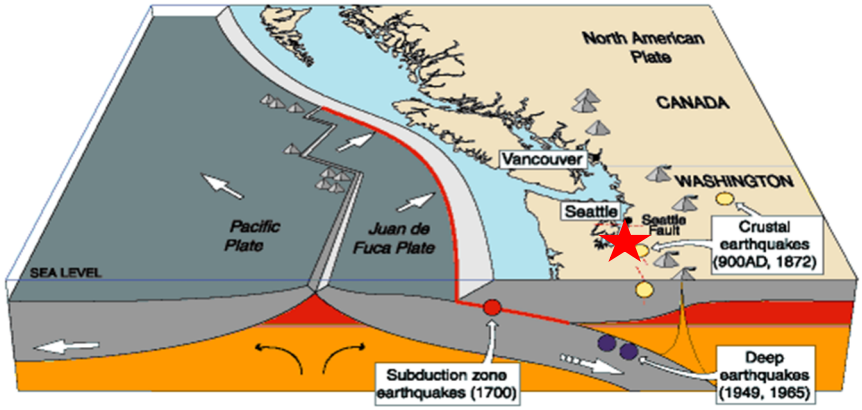

Figure 4.2: *Seattle Fault Map [10]*

4.2.2 Historic Seismic Activity in Seattle

The proximity of the site to the CSZ Interface, as well as the local Seattle Fault Zone, results in great seismic risk. In the past 30 years, the city of Seattle has endured four earthquakes above magnitude 4.9. In 1995, 1996, and 1997, shallow earthquakes struck near the city, with little to no damage reported. However, in 2001, the Nisqually Earthquake resulted in a magnitude 6.8 event, originating from tension in the subducting Juan de Fuca Plate [11]. This event was reported to have a similar mechanism to events that occurred in the region in 1949 and 1965. The Nisqually Earthquake produced widespread, strong ground shaking and caused an estimated $2 Billion of damage like that shown in **Figure 4.3** [11]. Resulting from the severe intensity, a dozen buildings were deemed unsafe, while a plethora of others faced significant damage, mostly due to the effects of liquefaction. The structural and geotechnical performance in the Nisqually Earthquake is important to study because it is within 60 miles of the existing hospital structure and the effected region had similar site conditions.

Figure 4.3: *Damage after the 2001 Nisqually Earthquake* [12,13]

4.2.3 Seismic Hazard Deaggregation

For the competition deliverable on seismicity (*Supplementary Material 4-3)*, the Cal Poly EERI SDC team was tasked with selecting a suite of five appropriate ground motions to which the original hospital and the original hospital with addition would be subjected. The remainder of this section provides the logic process used to identify the ground motions from the nine candidate options in *Supplementary Material 4-4* provided by the competition planning committee. The first step being to examine the site's seismic hazard, specifically to identify the distance and magnitude of predominate sources of the earthquakes.

With the provided method and givens from *Supplementary Material 4-3*, deaggregation plots were generated using United States Geological Survey's Unified Hazard Tool [14]. The data reported in the plots below aim to express the potential seismic hazards from the varying faults around the site to best predict seismic behavior of the structure. For simplification, the existing hospital structure is represented with a period of T = 1.0 sec, while the hospital with the addition is replicated with the plot for a structure with a period of T = 2.0 sec. The major hazard contributions from nearby thrust faults are highlighted in **Figures 4.4 and 4.5** in red, while the major hazard contributions from the CSZ are highlighted in green.

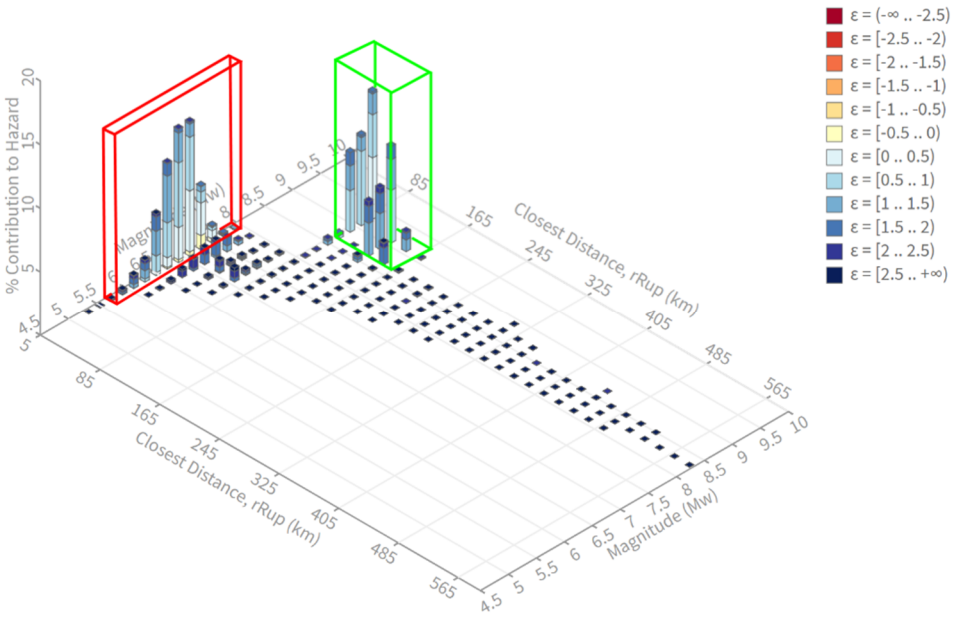

Figure 4.4: *Total Deaggregation Plot for T=1.0 Sec*

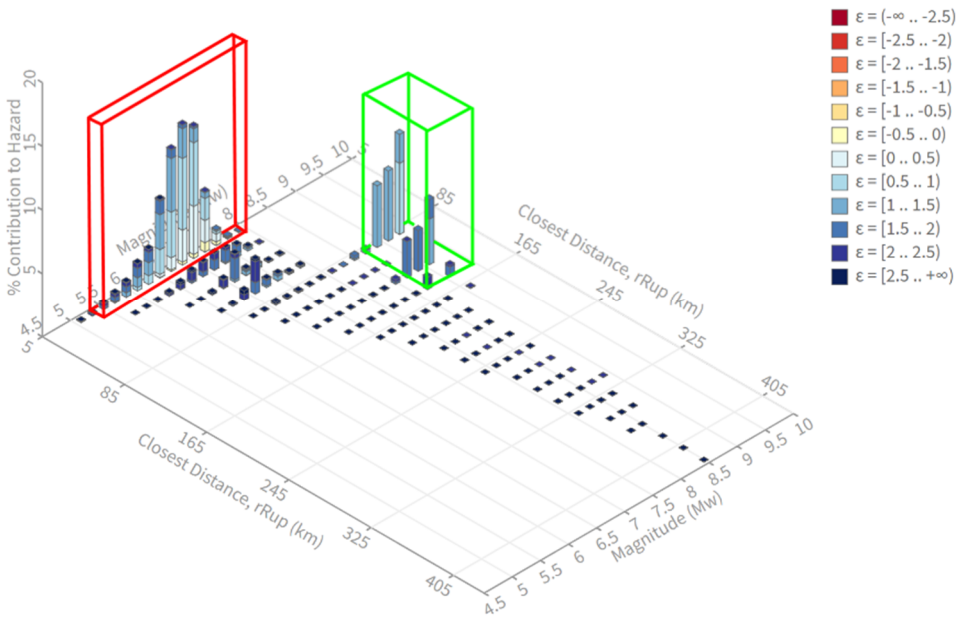

Figure 4.5: *Total Deaggregation Plot for T=2.0 Sec*

To further analyze **Figures 4.4 and 4.5**, the associated data file was exported to Microsoft Excel where values of magnitude, rupture distance, and binned percentage from each earthquake source were extracted. Then, values were categorized by rupture distance to distinguish hazard due to the nearby thrust faults from the CSZ Interface, allowing for a more in-depth comparison to the varying contributions represented in the deaggregation plots.

Table 4.1: Deaggregation Contribution to Seismic Hazard Summary						
Contributing Sources	T = 1.0 sec			T = 2.0 sec		
	m	r (km)	%	m	r (km)	%
Nearby Faults (<15 km)	6.82	10.12	57.94	6.92	9.98	50.36
Cascadia Subduction Zone Interface	9.01	104.55	32.65	8.99	107.3	45.51
Other Sources	7.17	62.83	9.42	7.27	62.84	4.13

Values reported for magnitude, m, and rupture distance, r, in **Table 4.1** were obtained using an average of source values. When averaging values in this regard, it is a more efficient method than running a multitude of ground motions through the structure. However, this does result in extremely generalized data that cannot not precisely predict a specific ground motion. Overall, this is an accepted approach due to the scope and timeline of the competition.

4.2.3.1 Deaggregation Analysis

While the overall percent contributions can be seen in **Table 4.1**, according to the United States Geological Survey's Unified Hazard Tool, the sources with the greatest contributions to hazards were attributed to a nearby fault for the idealized existing hospital structure and an interface fault for the hospital with the proposed addition [14]. Corresponding ground motions from the works of Chiou & Youngs [15] binned at the largest percentage for T = 1.0 sec, with a magnitude of 6.81 and a rupture distance of 9.45 km. Ground motions of this nature are responsible for intense shaking that diminishing quickly, causing a forceful shock to impact the structure. For T = 2.0 sec, Atkinson & Macias [15] predicted ground motions binned at the greatest value and had representative values with a magnitude of 8.97 and a rupture distance of 108.62 km. Earthquakes along the Cascadia Subduction Zone are responsible for deeper, larger events as they occur in subduction zones, where tectonic plates interact. These ground motions make up the most historic hazards that are likely similar to those that could impact the site.

4.2.4 Select and Scale Time Histories

4.2.4.1 Design Response Spectrum

A site-specific design response spectrum helps predict spectral accelerations for linear response of any given building period, which can be used to obtain earthquake-induced lateral forces on the structure. The design response spectrum in **Figure 4.6** was developed using values for the site from the ATC Hazard Tool [15] and ASCE 7-16 [1], as well as Python code output found in *Supplementary Material 4-5*, see **Appendix 4.2.4.1** for a summary table of values used. With inputs of S_{DS} and S_{D1}, Python script produces a response spectrum figure, as well as Microsoft Excel outputs that were used to produce **Figure 4.6**. From the site-specific design response spectrum, it was determined that the S_a of the existing hospital, with T = 1.0 sec equals 0.59 g which is greater than the expected spectral response of the hospital with the additional floors where the S_a value equals 0.29 g.

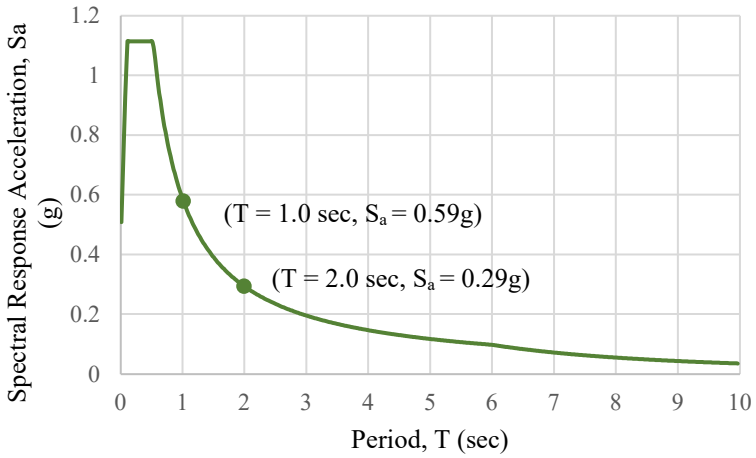

Figure 4.6: *Design Response Spectrum for Site*

4.2.4.2 Ground Motion Selection

In accordance with ASCE 7-16 Section 16.2.2 [1], "ground motions shall be selected from events within the same general tectonic regime and having generally consistent magnitudes and fault distances and shall have similar spectral shape to the target spectrum … the proportion of ground motions with near-fault and rupture directivity effects shall represent the probability that Maximum Considered Earthquake (MCE) shaking with exhibit these effects." Guidance from this section was taken into consideration when selecting from candidate ground motions found in *Supplementary Material 4-4*.

There are a number of methods to select and utilize historic ground motions to simulate potential seismic events. In this process, three critical parameters were considered. The first was the shear wave velocity ($V_{S,30}$) to appropriately consider soil type and its impacts to the frequency and duration of shaking during an earthquake. Next, considering the magnitude ensured the selected ground motion will result in a level of shaking that closely aligns with the predicted values. Finally, rupture distance was reviewed for fault classification and to ensure earthquake magnitudes could be compared without the need to account for significant energy dissipation. It is also important to ensure the rupture mechanism for the ground motion represents the same fault type as the site location.

All local ground motions that were selected were crustal reverse faults to align with the local Seattle thrust fault, described in **Section 4.2.1**, while all selected CSZ events corresponded to interfaces. While nearby faults account for the majority of the seismic hazard, only two seed motions appeared to reflect nearby faults (in all of the available options from *Supplementary Material 4-4*), while three more accurately reflect CSZ faults.

Table 4.2 summarizes the five selected seed motions with respect to the mean values from **Table 4.1** for a T= 2 sec (hospital with addition) for magnitude, m, rupture distance, r, and shear wave velocity ($V_{S,30}$) outlined in **Section 4.1.3**. Any variance less than 10% was accepted as a vital consideration that was used for selection.

Table 4.2 Selected Seed Motions with Percent Differences to Mean

Candidate Ground Motion	Magnitude	Percent Difference	Rupture Distance	Percent Difference	Shear Wave Velocity ($V_{S,30}$)	Percent Difference	Rupture Mechanism
	--	%	(km)	%	(m/s)	%	--
1978 Tabas, Iran	7.4	6.2	2	79	767	34	Crustal (Reverse)
1985 Nahanni, Canada	6.8	2.3	10	3.8	605	5.5	Crustal (Reverse)
2011 Tohoku, Japan	9	0.1	64	41	593	3.4	Subduction (Interface)
2010 Maule, Chile (ANTU)	8.8	2.3	65	40	621	8.3	Subduction (Interface)
2001 Arequipa, Peru	8.4	2.3	77	29	573	0.1	Subduction (Interface)

4.2.4.3 Seed Motion Selection

To relate recorded ground motions more accurately to that of the site in Seattle, the selected motions needed to be scaled to closely align with the design response spectrum found in **Figure 4.6**. Per the competition planning committee, in order to create more uniformity across competition teams, the previous ground motions analyzed in **Section 4.2.4.2** will not carry through to the modelling stage. Using the Pacific Earthquake Engineering Research (PEER) Ground Motion Database [16] and following the inputs outlined in *Supplementary Material 4-3*, a comprehensive list of seed ground motions with reported characteristics was obtained, see *Supplementary Material 4-6*. Among those listed, the 1992 Cape Mendocino seed ground motion was selected to scale to the four seed motions required by the SLC, see **Figure 4.7**. This was the case because the 1992 Cape Mendocino motion has parameters consistent with the site as discussed in **Section 4.2.4.2** (a similar $V_{S,30}$, then approximate magnitude event, followed by a close rupture distance to the mean event with a T = 2 sec from **Table 4.1**).

Data for this ground motion was extracted from *Supplementary Material 4-6* and transferred to *Supplementary Material 4-7*, a Microsoft Excel file provided by the competition planning committee that contained the other selected ground motions. The calculated spectral accelerations from the design response spectrum in **Section 4.2.4.1** were also input into the file. Using all this data, the plot of **Figure 4.7** was generated to display the unscaled response spectrums of the provided ground motions against the site-specific design response spectrum.

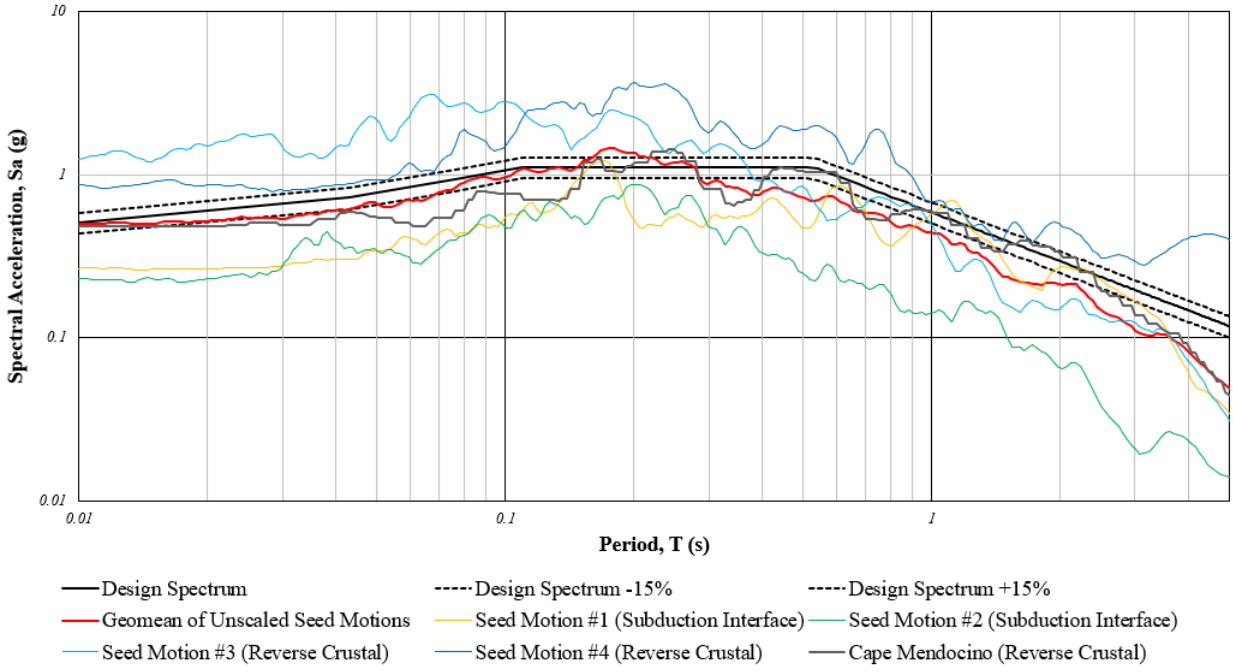

Figure 4.7: *Unscaled Pseudo-Spectral Acceleration Response*

As shown above in **Figure 4.7**, the peaks and valleys of the different motions are not aligned. Scaling was necessary to match the conditions of the selected seed motion, 1992 Cape Mendocino, to other seed motions provided and to the design response spectrum from **Figure 4.6**. Scaling was accomplished by applying a factor to the spectral acceleration to make the plot match the design spectrum. The final scale factors can be seen in **Table 4.3** and **Figure 4.8**. The modifications that occurs between **Figure 4.7** and **Figure 4.8** are crucial to the design process since the ground motions are more likely to represent similar conditions when used in a computer-generated building model. This can be used to better predict spectral accelerations at any given period for the proposed structure.

Table 4.3: Ground Motion Scale Factors		
Seed Motion Name	**Rupture Mechanism**	**Scale Factor**
Seed Motion #1	Subduction Interface	1.2
Seed Motion #2	Subduction Interface	3.4
Seed Motion #3	Reverse Crustal	2.0
Seed Motion #4	Reverse Crustal	0.75
1992 Cape Mendocino	Reverse Crustal	1.1

Figure 4.8: *Scaled Pseudo-Spectral Acceleration Response*

5 EXISTING BUILDING MODEL AND PERFORMANCE ASSESSMENT

After the site conditions were determined, a performance assessment of the existing hospital structure was conducted by creating a numerical model using commercial structural analysis software ETABS 19 [17], in order to understand the building's baseline performance before the vertical addition. The original steel structure was represented by a scaled balsa wood model which was evaluated by carrying out a modal analysis and four-time history analyses, using the ground motions provided by the competition planning committee.

5.1 MODELLING ASSUMPTIONS

In *Supplementary Material 5-1*, teams were instructed to assume the balsa wood material properties shown in **Table 5.1** and utilize given modelling assumptions related to base and connection fixity, diaphragm stiffness, modal damping, among others. As part of the deliverable, students were asked to evaluate and comment on the appropriateness of these assumptions, for the original full-scale steel structure and the scaled balsa wood model. The remainder of this section contains an assessment of the accuracy of the given assumptions in translating the design and construction of the existing structure to a computer model.

Table 5.1: Design Properties for Low- to Medium-Density Balsa Wood

Fb	Ft	Fv	Fc	E	Emin	Density
2000 psi	1200 psi	200 psi	900 psi	600,000 psi	350000 psi	8 lb/ft³

5.1.1 Base Fixity and Member Connections

The base of the columns were required to be modelled as fixed and members as continuous such that all connections were moment resisting. This assumption lends itself well to a balsa wood model in which all connections are epoxy glue joints, including the columns to base. However, this approach is invalid for a real steel structure. In this case, it would be more appropriate to assume columns are pinned at the base, with modifications of nonlinear springs to account for the behavior of soil and foundation pile interaction, see **Section 4.1.2**. Further, braces are pinned at intersections and beams are fixed. Complete fixity is difficult to achieve in any real-life structure and should only be used in small-scale models, like those made of balsa wood [18].

5.1.2 Poisson's Ratio

The given Poisson ratio value of 0.3, utilized in the model, is valid for balsa wood. This value is very similar to A36 steel with a Poisson's ratio of approximately 0.32 [19]. For this reason, the given value can be used for both a balsa wood as well as a steel model.

5.1.3 Damping Ratio

The given equivalent viscous damping value of 2.5% was specified for all modes. While it can be difficult to predict damping, it has a strong influence on the dynamic behavior of a structure. Damping of structures cannot solely be based on a linear model, so frictional damping must be considered to include imperfections of the material consistent with failure mechanisms [20]. When the structure is excited and as energy is dissipated, the structural damping increases. This stated value of 2.5% seems low based on a sensitivity analysis conducted by the team that indicated that as the damping ratio increases, member forces decreased. Thus, a higher percent damping will result in smaller design forces, ensuring a level of conservatism with the provided 2.5%, since amongst the wide range of accepted values for varying building materials, a steel moment frame is accepted to have a damping value of 5% [21].

5.1.4 Diaphragms

The given modelling assumption of a flexible diaphragm implies that horizontal lateral force resisting elements (floors or roof) are idealized to behave like a simply supported beams. This assumption requires that specific conditions must be met, outlined in ASCE 7-16 Section 12.3.1.1 [1]. While flexible diaphragms often apply to wood structures, the balsa wood model has a relatively high degree of fixity in the connections and therefore the overall floor system is anticipated to behave in a more rigid manner. The flexible diaphragm assumption is also not realistic for a steel structure that is fabricated with either a concrete slab, or concrete-filled metal deck. The modeling assumption alters whether loads are proportioned to vertical lateral force resisting elements according to tributary area, as done in the scale balsa wood model, or relative stiffness as what should be done for a steel structure [22].

5.1.5 Loading

The specified superimposed dead load of 1.44 pounds per square foot (psf) was applied as nodal loads in the negative z-direction based on each joint's tributary area. This nodal load was also assigned as masses in the x and y-directions to ensure each node would be excited by the ground motion without increasing the stiffness of the structure.

5.2 ANALYSIS

With the modelling assumptions outlined in **Section 5.1**, in conjunction with plans and elevations found in *Supplementary Material 5-2*, dead loads outlined in **Section 5.1.5** and time histories from *Supplementary Material 5-3* were applied to a 10-story ETABS [17] model. The results of the modal and linear time history analyses of the existing structure are reported in this section.

5.2.1 Modal Analysis

The periods of the first three modes of the ETABS [17] balsa wood model are: T_{M1} = 0.148 seconds, T_{M2} = 0.092 seconds, and T_{M3} = 0.069 seconds. The dominant mode shapes of were mainly torsional resulting from the fact that the center of rigidity is nearly aligned with the west (orange) face of the structure, as shown in **Figure 5.1 and 5.2**. The dominant shape of the second mode was strictly translational in the UX (East-West) direction, as shown in **Figure 5.2(b)**. The third dominant mode shape exhibits double-bending along the building height as shown in the 3D view in **Figure 5.2(c)**, and a combination of torsion and UY (North-South) translation in the plan view.

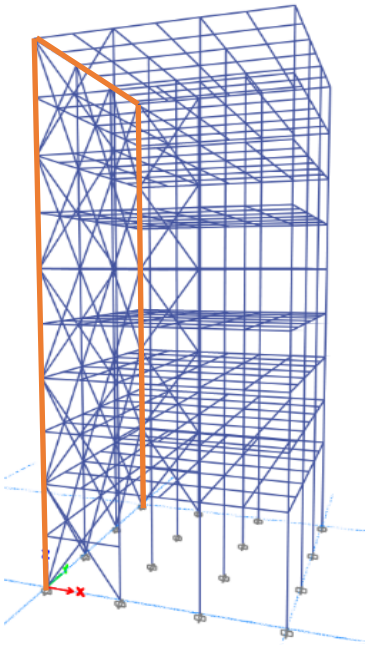

Figure 5.1: *ETABS Model of Existing Structure*

While only three modes are presented in this report, it should be noted that per ASCE 7-16 Section 12.9.1.1 the analysis shall include a minimum number of modes to obtain a combined modal mass participation of at least 90% of the actual mass in each orthogonal horizontal direction [1]. The first five modes must be included in analysis in UX (92.03%) and the first nine modes for the UY direction (91.14%). It is typical for a structure to have need at least three modes to achieve this participation, two translational (UX and UY) and one rotational [23]. Considering this structure is 20 stories, having more mode shapes needed to meet the 90% threshold is not surprising.

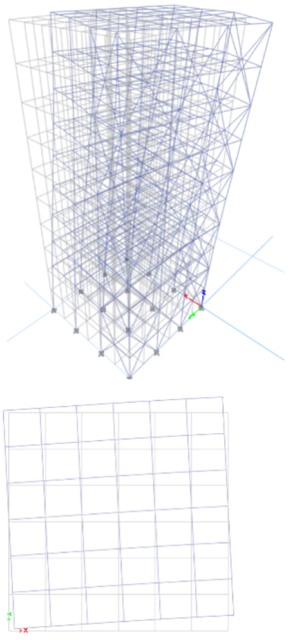

Figure 5.2(a): *Mode 1*

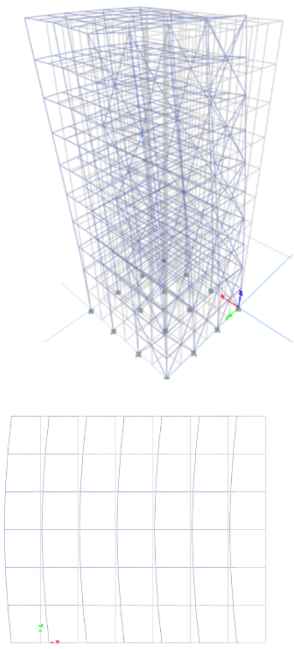

Figure 5.2(b): *Mode 2*

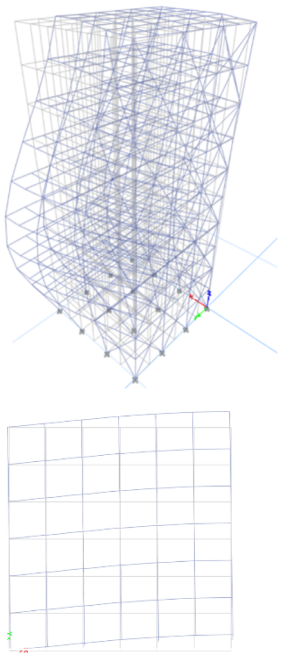

Figure 5.2(c): *Mode 3*

5.2.2 Linear Time History Analysis

5.2.2.1 Applied Loads

The remaining analysis of the structure will be carried out using four scaled ground motions provided by the competition, found in *Supplementary Material 5-3*. **Figure 5.3** contains the four scaled ground motions (TH1-TH4), plotted in MATLAB [24], used to conduct the linear time history analyses to predict the structure's seismic response. These ground motions vary in duration and amplitude and are intended to simulate both short, intense events as well as longer events with multiple shocks. Since the structure is being modeled as a scale balsa wood structure, the allowable stress design (ASD) factored load combinations from ASCE 7-16 [1] were used with dead and earthquake loads being applied to the model. The subsequent sections examine the interstory drifts and demand forces that were extracted.

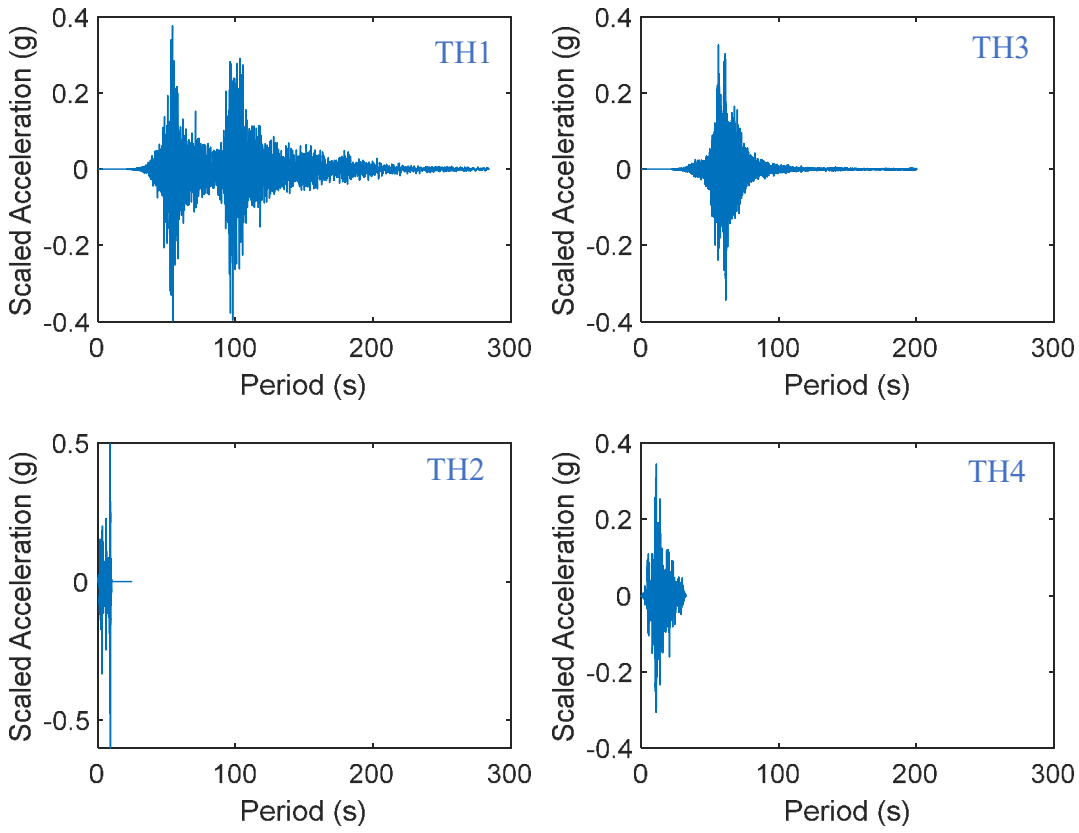

Figure 5.3: *Plots of Applied Time Histories*

5.2.2.2 Seismic Response

5.2.2.2.1 Interstory Drift

The maximum relative translational displacements between different story levels can be seen in **Figure 5.4** These values are well below 5% for the structure, which is considered the maximum threshold for a controlled response of structural damage after a seismic event [25]. The maximum drift ratios occurred in the load combination 1.0 D + 0.7 TH1 in the first ground motion which had the longest duration with two jolting shocks, seen in **Figure 5.3**.

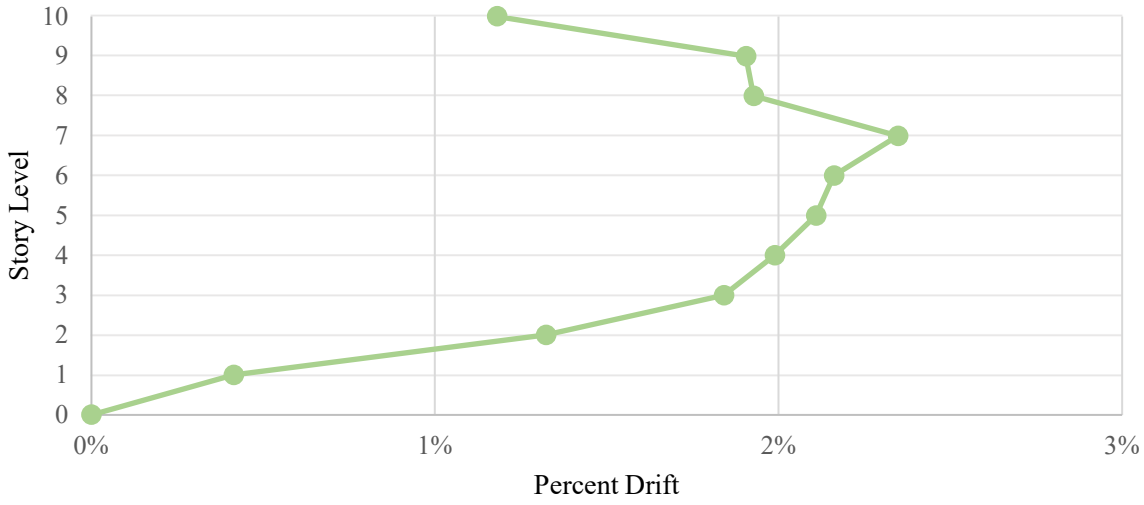

Figure 5.4: *Maximum Interstory Drift Ratios for Existing Structure*

5.2.3.2 Member Forces

Maximum member forces were extracted from ETABS and reported as demand values. Capacity values were then calculated using the NDS [3] and are reported in **Table 5.2**, see **Appendix 5.2.3.2**. These maximum loads were utilized to calculate member stresses listed in **Table 5.3,** then compared to the calculated capacities. It can be seen in **Table 5.4** that these values for axial, shear, moment, and combined were all well below the strength capacity failure at a ratio of 1.0. Similar to interstory drift, the first ground motion resulted in the highest force demand.

Table 5.2: Applicable Material Properties

Member	Area	Unit
Column	0.040	in^2
Brace	0.026	in^2
Beam	0.014	in^2

Table 5.3: Calculated Capacities

Fc'	905	psi
Ft'	2880	psi
Fv'	320	psi
Fb'	4800	psi

Table 5.4: Maximum D/C Ratios for Worst Case Time History		
	Member	D/C Ratio
P	Beams	0.307
	Braces	0.345
	Columns	0.608
V	Beams	0.055
	Braces	0.009
	Columns	0.019
M	Beams	0.160
	Braces	0.036
	Columns	0.070
M + P_T	Columns	0.257
M + P_C	Columns	0.313

6 VERTICAL ADDITION

With guidance from the Seattle Mayor, the existing hospital structure was selected for a 10-story vertical extension with a sloped West face, doubling its patient capacity. Per *Supplementary Material 5-1* it was not permitted to modify the existing floors of the hospital at this point. With this in mind, the following design focuses on the bracing scheme of 10 new stories in accordance with *Supplementary Material 6-1*.

6.1 STRUCTURAL PRECEDENTS

Faced with the design challenge of a tapered floor plan in the schematic design phase, it was important to look towards structural precedents to understand how to transfer load from the new vertical extension into the existing structure.

6.1.1 U.S. Bank Center | Milwaukee, WI

Completed in 1973, the U.S. Bank Center in Milwaukee, Wisconsin is an example of a core-and-outrigger system [26]. For purpose of the addition design, the outrigger used in this building will be applicable. In **Figure 6.1**, the stiff outrigger trusses were placed at mechanical levels that were linked with belt trusses to help engage all of the columns in the resistance of lateral loads [26]. This system allows for an increase in overall lateral stiffness that works to tie the entire structure together. In the addition, the use of a belt truss was thought to tie the existing bracing layout with the upper stories to help performance in a seismic event.

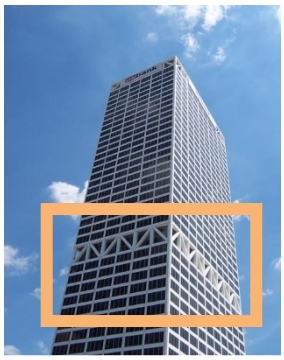

Figure 6.1:
U.S. Bank Center [27]

6.1.2 425 Park Avenue Tower | New York City, NY

Figure 6.2:
425 Park Avenue [29]

The 425 Park Avenue Tower replaces a 32-story building first constructed in the 1950s. Retaining 25% of the existing structure at the base, the newly reconstructed building now stands at 47-stories [28]. The design of the sloped "V" and tripod columns are of interest to the team's design because they slant to accommodate the tapered façade [28]. This is similar to the hospital structure where the floor plan tapers by using sloped columns and braces to eliminate cantilevers and allow for a more open floor plan. Additionally, the 425 Park Avenue Tower building is an adaptive reuse project that serves as a clear example that the constructability of the vertical addition to the existing hospital could be accomplished if it were erected in steel.

6.2 ARCHITECTURAL CONSIDERATIONS

6.2.1 Layout

The combination of a belt truss and sloped column work to accommodate the architecture. The function and comfort of the hospital were of the utmost importance for staff and patients alike when considering the architectural design outlined in *Supplementary Material 6-2*. The large hallway that circles the middle of the floor plans shown, helps to create steady circulation while allowing for proper social distancing, as seen in **Figure 6.3(a)** and **Figure 6.3(b)**. Placing smaller patient rooms on the exterior allows for privacy and maximum natural light, promoting a healing environment for patients. With the change in floor plan size as the building tapers, it was key to keep a consistent layout that would allow for accessibility. In **Figure 6.3(c)** and **Figure 6.3(d)**, produced with Revit [18], the grey regions indicate storage space beneath sloped ceilings that appear at each level of the addition. The green and orange shaded regions shifts right in parallel with the grey region as each of the upper levels' floor area is reduced, per the architect, due to limited floor-to-ceiling clearances to ensure every room was adequate to serve as an operating space if necessary. While the floor plans vary, they maintain the same base allowing for steady flow throughout the levels as patients and medical staff navigate through the hospital.

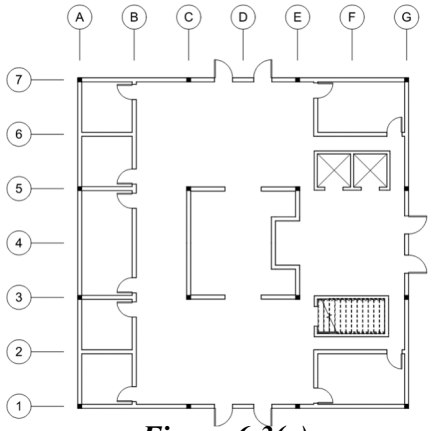

Figure 6.3(a):
Lobby Floor Plan (Level 1)

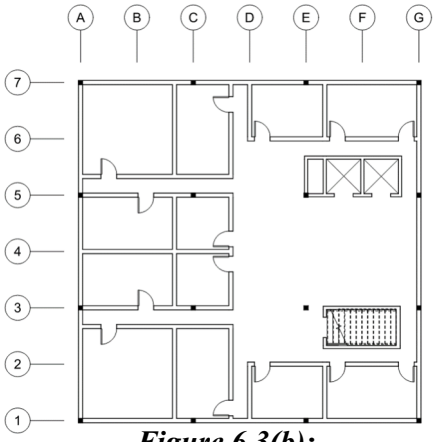

Figure 6.3(b):
Typical Existing Floor Plan (Levels 2-10)

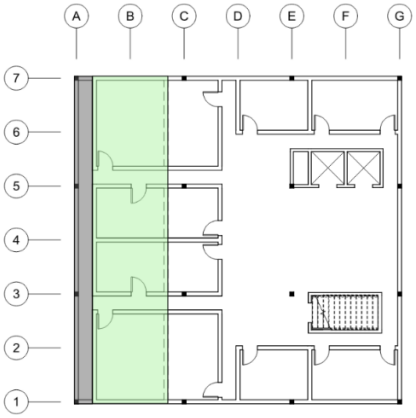

Figure 6.3(c):
Addition Floor Plan (Levels 11-15)

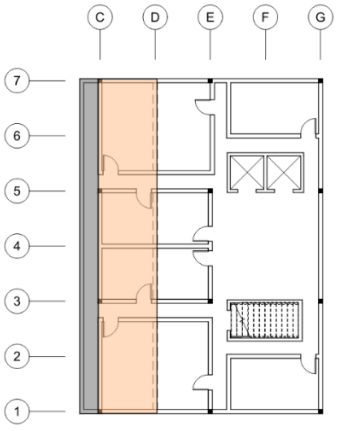

Figure 6.3(d):
Addition Floor Plan (Levels 16-19)

6.2.3 Sustainability

In striving for LEED accreditation, key aspects for design included materials and resources, indoor environmental quality, energy and atmosphere considerations, along with water efficiency [31]. Reusing as much material as possible from the existing building and ensuring new materials were responsibly sourced and free of harmful chemicals was crucial to the planning. Proper air flow and purification as well as well as adequate sunlight and shading in each room were important to achieve patient health and comfort objectives. Energy efficient fixtures and appliances work to keep the operation carbon impact low [31].

6.2.3 Final Design

Figure 6.4 is the final rendering of the 20-story steel structure with a glass building envelope and grey mesh façade with orange lining. Inspired by the trendy neighborhood site near the Olympic Sculpture Garden, the bold colors and organic forms seen throughout wrap around the hospital in a façade that allows for fantastic 360-degree views of Elliot Bay, while setting a striking precedent for the future of modern hospitals.

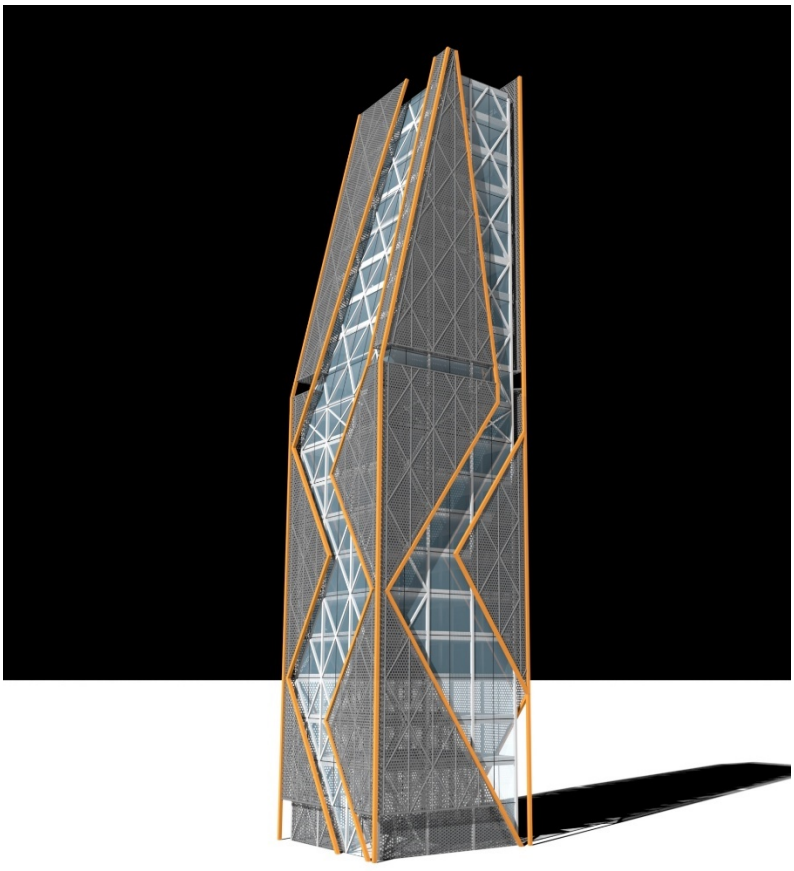

Figure 6.4: *Final Architectural Rendering*

6.3 ADDITION FINAL DESIGN

6.3.1 Design Iterations

Once the architectural criterion was met, three design options for the vertical extension were investigated using ETABS [17]. These design option models were created with varying brace layouts and member sizes within the constraints described in *Supplementary Material 6-1*. **Figure 6.5** shows the bracing layout for Iteration 1 and 2, where Iteration 2 has slightly smaller member sizes in the hopes of reducing seismic weight. **Figure 6.6** is the bracing layout for Iteration 3, where braces were removed from the East side of Iteration 1 for weight and stiffness concerns.

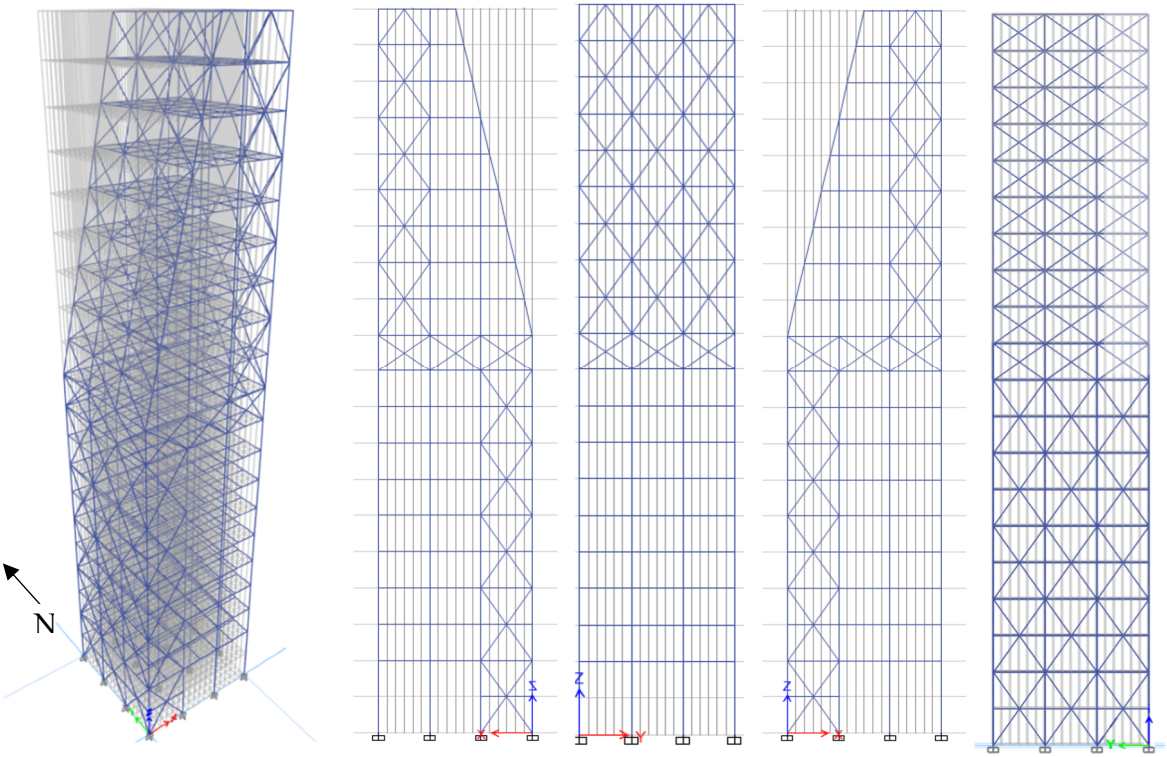

Figure 6.5: *Iteration 1 & 2 Layout for Addition*

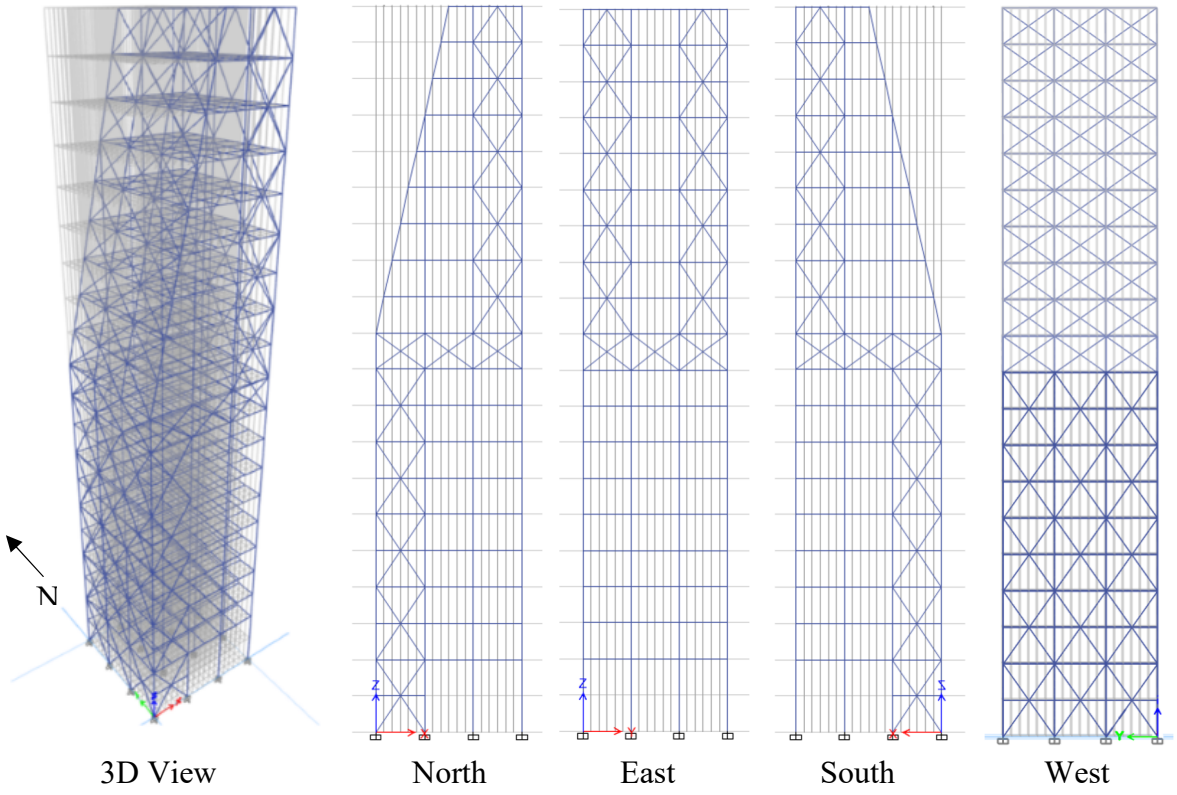

Figure 6.6: *Iteration 3 Layout for Addition*

The effectiveness of each design was determined by maximum displacements from **Table 6.1** and minimum demand forces from **Table 6.2**. Values in blue were deemed an independent success for that iteration, meaning that the value for either displacement or force was desired over the other iterations. Orange values represent a shared success, in which all iterations produced the same value for either displacement or force.

Table 6.1: Comparison of Design Iteration Drifts (inches)			
	Iteration 1	Iteration 2	Iteration 3
TH 1	0.615	0.686	0.764
TH 2	0.676	0.780	1.099
TH 3	0.523	0.608	0.772
TH 4	1.101	1.140	1.064

Table 6.2: Comparison of Design Iteration Demand Forces										
		P	V	M	P	V	M	P	V	M
		kips	kips	kip-ft	kips	kips	kip-ft	kips	kips	kip-ft
		Iteration 1			Iteration 2			Iteration 3		
Beams	TH1	0.009	0.001	2.92E-05	0.011	0.001	4.37E-05	0.009	0.001	3.93E-05
	TH2	0.008	0.001	2.06E-05	0.009	0.001	2.72E-05	0.01	0.001	0.0001
	TH3	0.006	0.00036	0.0001	0.007	0.000483	0.0001	0.007	0.001	0.0001
	TH4	0.013	0.001	0.0001	0.013	0.001	0.0001	0.01	0.001	0.0001
Braces	TH1	0.025	0.000149	2.41E-05	0.027	0.000169	2.60E-05	0.025	0.001	0.0001
	TH2	0.016	0.00065	2.13E-05	0.017	8.95E-05	1.54E-05	0.019	0.001	0.0002
	TH3	0.013	0.000121	0.000042	0.014	8.91E-05	2.01E-05	0.014	0.001	0.0001
	TH4	0.025	0.000262	0.000039	0.024	1.27E-04	2.21E-05	0.019	0.001	0.0002
Columns	TH1	0.045	0.001	0.0001	0.053	0.001	0.0001	0.043	0.001	0.0001
	TH2	0.049	0.001	0.0001	0.052	0.001	0.0001	0.056	0.001	0.0002
	TH3	0.036	0.000433	0.0001	0.039	0.001	0.0001	0.039	0.001	0.0002
	TH4	0.079	0.001	0.0002	0.076	0.001	0.0002	0.054	0.001	0.0002

Iteration 1 had the most independent successes when looking at both drift and demand forces. At this stage in the design, the brace layout of Iteration 1 was selected for the vertical extension as it works to tie the existing structure to the addition with the belt truss between the 10th and 11th story. To provide support for the taper and eliminate cantilever decks, sloping columns and braces were placed on the West face. To shift the center of rigidity away from this face, bracing was placed on the corners of the remaining sides. This design aims to connect the existing structure with the addition, while maintaining ensuring a continual load flow and architectural appeal.

7 SEISMIC RETROFIT IMPLEMENTATION AND PERFORMANCE ASSESSMENT

7.1 EVALUATION OF ADDITION WITH ORIGINAL BASE STORIES

Once the vertical addition design was chosen, alterations to the existing structure were permitted per *Supplementary Material 7-1*. Preliminary analyses that had already been carried out for comparing the vertical addition design options in **Section 6.3** did not have provided benchmark values to indicate the limit states for a safe design, the selected design seen in **Figure 6.6** was solely decided on the performance of the iterations against each other. However, during this retrofit phase, thresholds were provided to ensure the performance of the structure.

7.1.1 Time History Analysis

7.1.1.1 Interstory Drift

A similar set of time history analyses (TH1-TH4) that was completed for the existing structure in **Section 5.2.3** were also carried out on the model with the vertical addition. The maximum interstory drift limit of 5%, seen in **Figure 7.1**, was surpassed. This means that in the event of an earthquake, the drift between two adjacent floor levels is significant due to the relative change in stiffness and there is more substantial damage risk. In contrast to the existing structure where the first ground motion (TH1) controlled, here the fourth time history (TH4) produced the largest interstory drifts. This ground motion represents the shortest earthquake with a greater proportion of high accelerations.

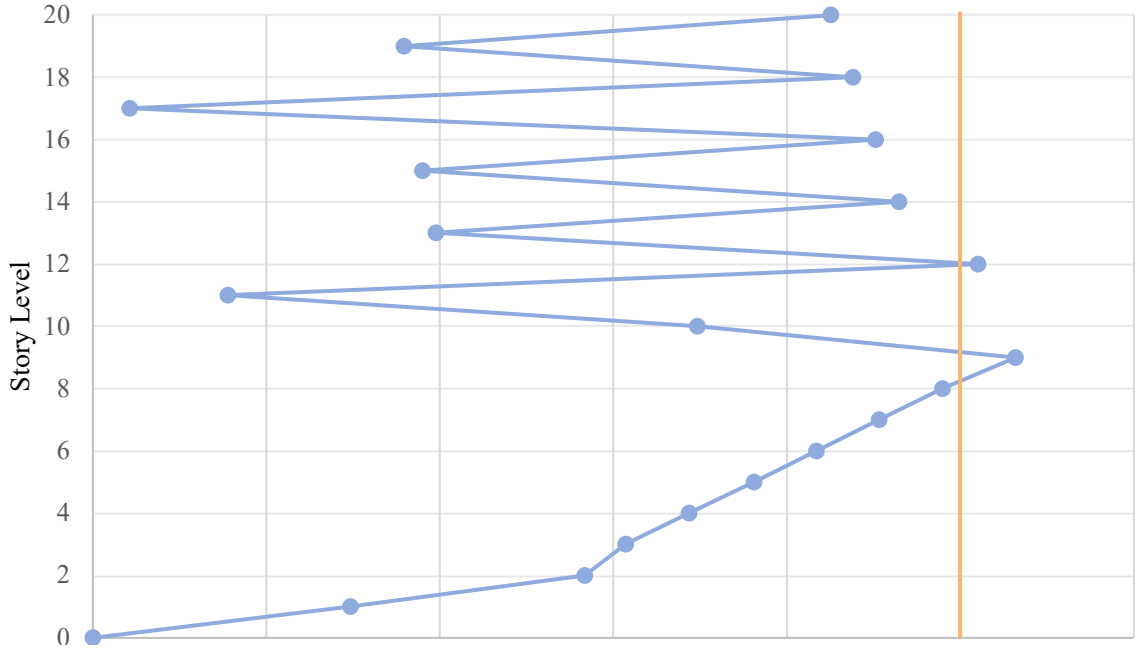

Figure 7.1: *Maximum Interstory Drift Ratios for Existing Structure with Addition*

7.1.1.2 Member Forces

From the time history analyses, maximum forces were extracted from ETABS [17] and turned into demand stresses, then compared to the capacities found in **Appendix 5.2.3.2**. As seen in **Table 7.1**, more than one member surpassed its strength limit. Members that failed here were mainly sloped columns of the addition, as they are taking a larger proportion of axial, and also combined forces, due to their angled orientation.

Table 7.1: Maximum D/C Ratios for Worst Case Time History

	Member	D/C Ratio
P	Beams	0.691
	Braces	0.777
	Columns	**1.519**
V	Beams	0.326
	Braces	0.034
	Columns	0.117
M	Beams	0.253
	Braces	0.088
	Columns	0.188
M + P_T	**Columns**	**1.226**
M + P_C	**Columns**	**1.461**

7.2 EVALUATION OF ADDITION WITH RETROFITTED BASE STORIES

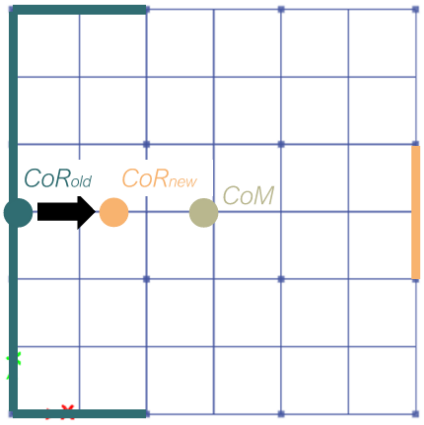

Figure 7.2:
Shift in Center of Rigidity to Center of Mass

Once the assessment of the addition with the original base structure was complete, the competition rules now permitted engineering teams to begin modifying the base structure and its asymmetric brace layout. Due to the excessive interstory drift and member demand-to-capacity ratios identified in **Section 7.1**, the team began designing a retrofit scheme that both modifies the members and bracing scheme of the addition and the existing structure. The priority of this redesign and retrofit was to reduce interstory drift, eliminate member failure, and alleviate susceptibility of the overall structure to torsion. This was achieved by adding a series of vertical braces from the base to the 10th story on the East side, allowing for vertical continuity of stiffness along the building height. These braces, opposite the existing braces, work to shift the center of rigidity away from the West side of the

structure to more closely align with the center of mass, as seen in **Figure 7.2**. Along with the updated brace layout, the column dimensions of the vertical addition were increased from 0.20 inches to 0.22 inches (modification made for this report after the competition ended, based on further analysis). While this exceeds the member size permitted per *Supplementary Material 6-1*, it is necessary in order for the design to meet the engineering criteria discussed previously. This new value for member size resulted from more in-depth examination of combined forces particularly in sloping columns requiring the increased member size that allows for a greater member capacity in excess of demands.

7.2.1 Constructability

While the numerical model represents a balsa wood structure, and as not specified by the competition, should this design be erected, it would likely be made of steel. This material selection is on account of the high density of braces used in design. In the balsa wood structure, these new braces could be added with correctly sized members with small balsa wood squares glued to the exterior of the connections as gusset plates. These connections can be easily replicated with precision in a model structure.

In terms of a full-scale building, these braces would be designed as steel and connected with gusset plates. Since all braces will be placed on the exterior of the existing structure, they can be implemented by removing the existing façade and welding gusset plates to the existing steel columns. Once these braces are added, the upper addition can begin construction, ensuring that the vibrations will not interfere with the medical equipment and procedures. Communication with hospital staff will be vital to complete this project safely. To create a continuity for load flow, it would be likely that a new layer of concrete would need to be poured to incorporate the gusset plate and get full use. Overall, the sequence of demolition and construction will be vital to keep the hospital functioning during construction. For a full idealized construction sequence of the retrofit and remodel, see **Appendix 7.2.1**, Approximation of Construction Schedule and Sequence.

7.3 FINAL RETROFIT AND REMODEL DESIGN

7.3.1 Performance Assessment

Figure 7.3 provides a comparison of the interstory drift for the existing, addition, and retrofitted structure. The final retrofitted model greatly decreased the interstory drift ratios for the existing structure with addition by nearly half and well below the 5% drift limit.

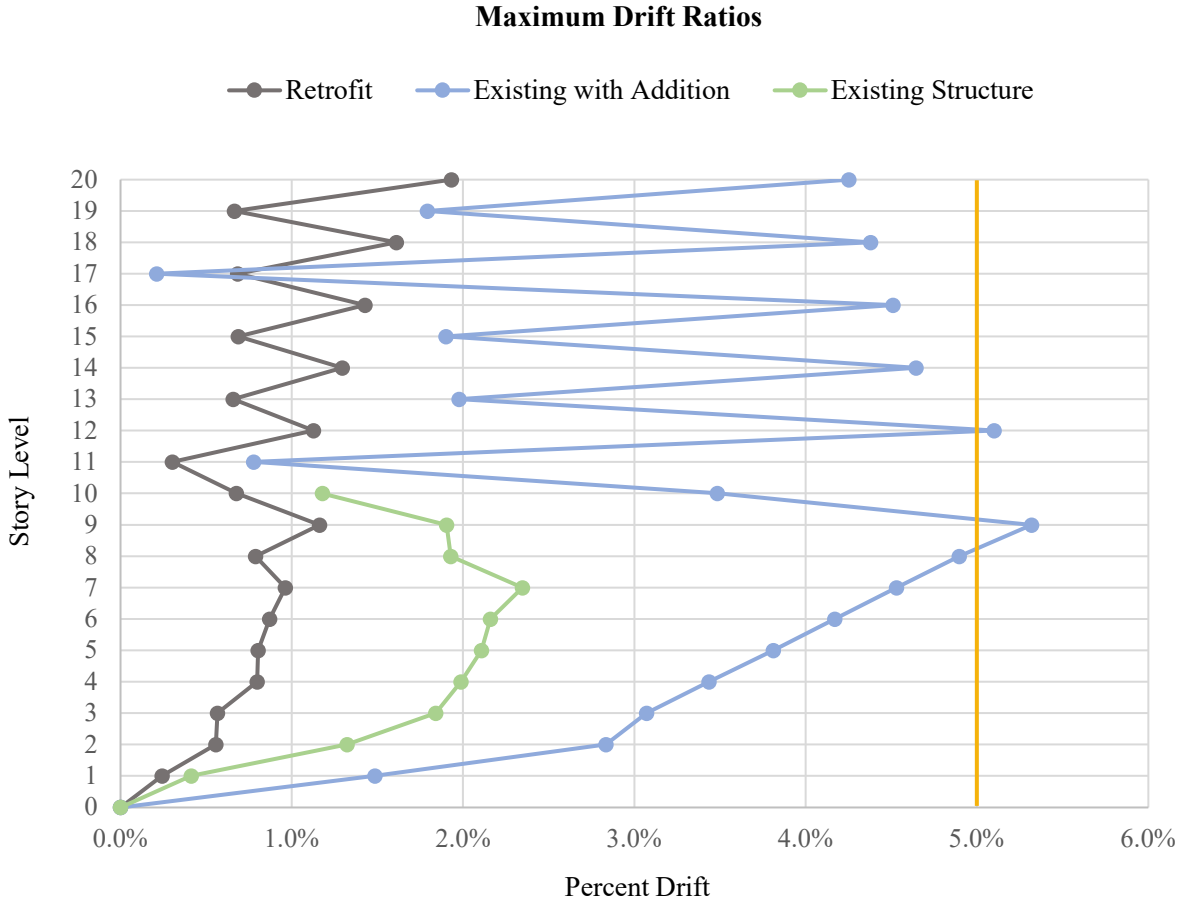

Figure 7.3: *Comparison of Maximum Interstory Drift Ratios*

7.3.2 Final Drawings

The completed model of the existing structure with addition and modified retrofit and redesign can be seen in **Figure 7.4 and 7.5** on sheets S2.1 and S3.1 of the drawing package submitted as a competition deliverable. This finalized ETABS model has all members passing their respective capacity checks, with the greatest D/C ratio of 0.88 in a base column and has all interstory drift ratios below 5%.

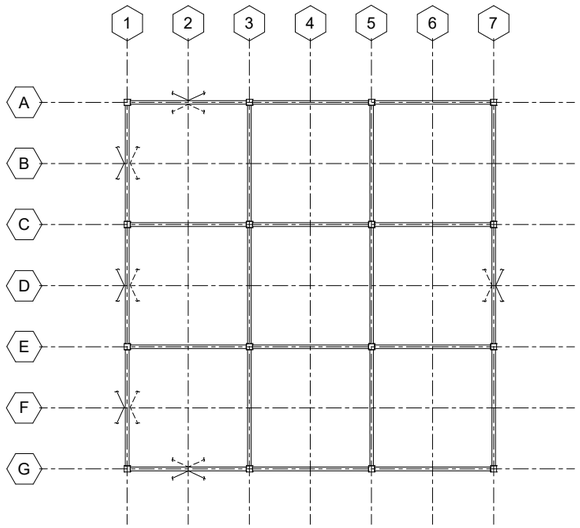

1 FLOOR 9

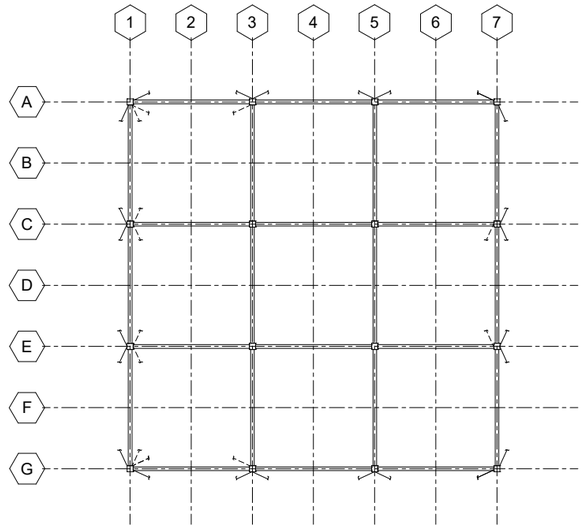

2 FLOOR 10

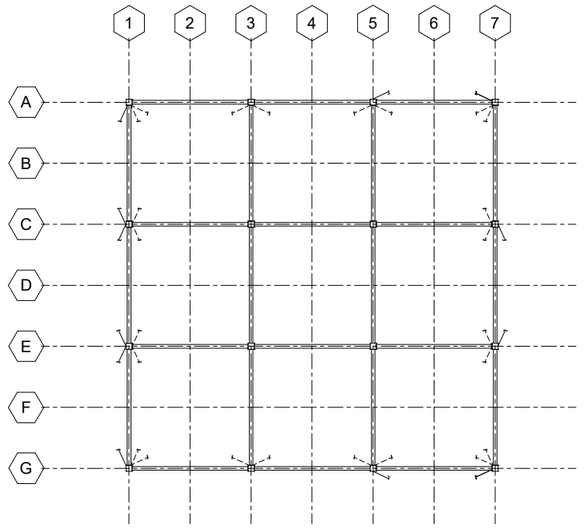

3 FLOOR 11

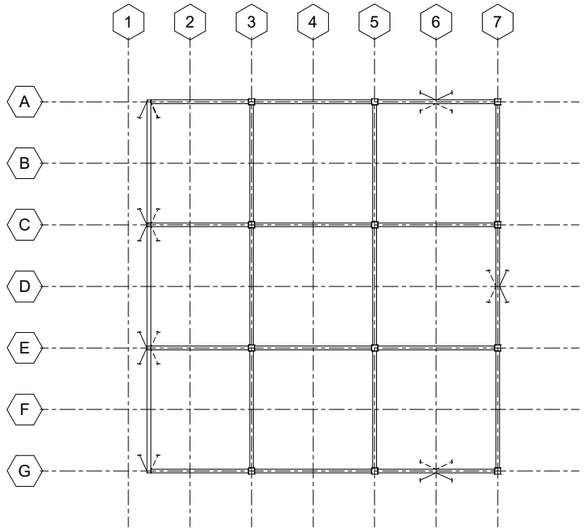

4 FLOOR 12

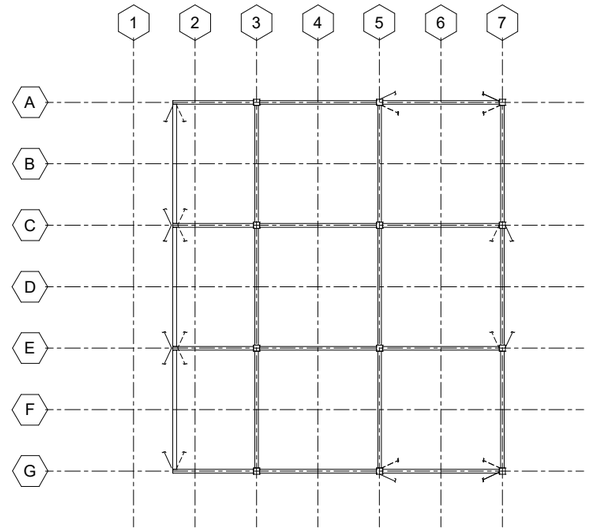

5 FLOOR 13

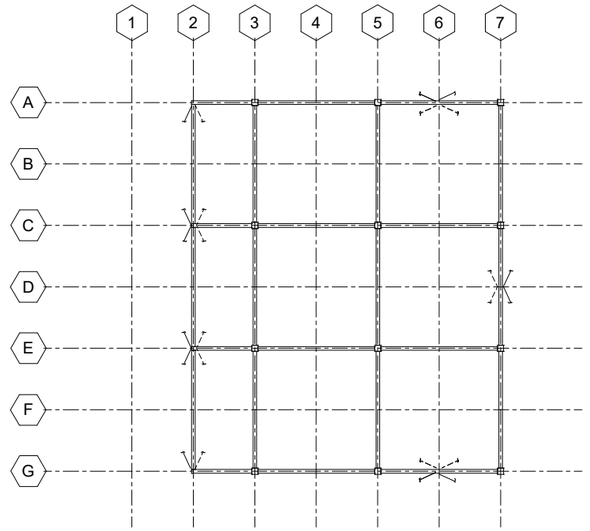

6 FLOOR 14

Figure 7.4: *S2.1 - Final Structural Floor Plans*

1 GRAND AVE
SAN LUIS OBISPO, CA 93407

STAMP:

PRINTING		
No:	DESC:	DATE:

REVISIONS		
No:	DESC:	DATE:

SHEET NAME:
FLOOR PLANS

SHEET No.:
S2.1

DRAWN BY:

SCALE:

SUBMITTAL DATE:
4/11/2021 4:13:17 PM

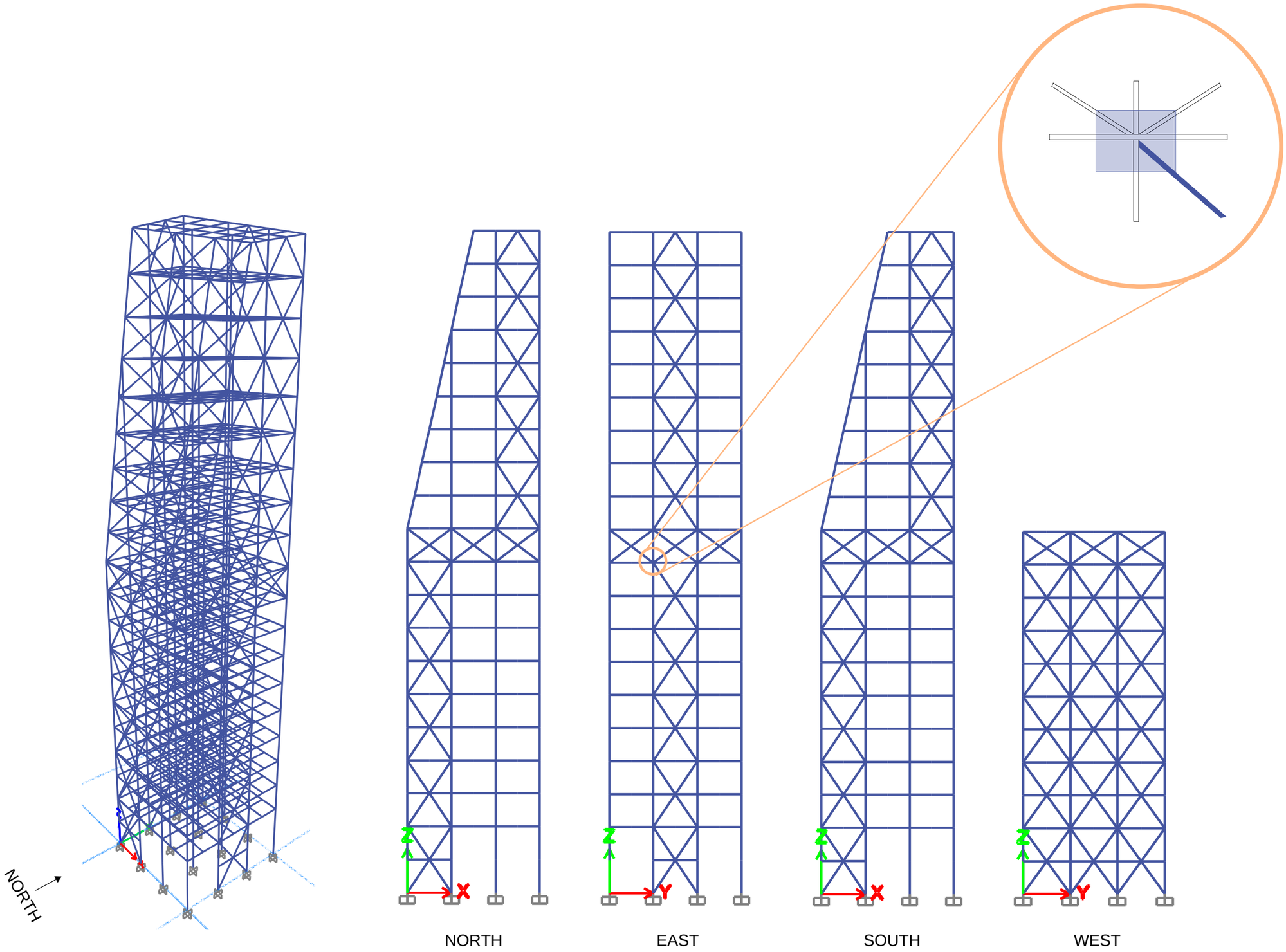

Figure 7.5: *S2.2 - Final Structural Elevations and Connections*

EERI

EERI Student Leadership Council

ARCE

1 GRAND AVE
SAN LUIS OBISPO, CA 93407

STAMP:

PRINTING		
No:	DESC:	DATE:

REVISIONS		
No:	DESC:	DATE:

SHEET NAME:
ELEVATIONS & CONNECTION

SHEET No.:
S3.1

DRAWN BY:

SCALE:

SUBMITTAL DATE:
4/11/2021 4:13:17 PM

8 DESIGN IMPACT

The impact of a redesign and seismic upgrade to a hospital structure can better equip the facility to remain functional during and after an earthquake helping to maintain the global, cultural, social, and economic vibrancy of the surrounding community that existed prior to a hazard event.

8.1 PUBLIC HEALTH AND SAFETY

Of the utmost importance for any structural engineering project, especially critical infrastructure like a hospital, is the safety of the occupants and resiliency of the community. It is the responsibility of a professional to design, analyze, and construct buildings that house and protect citizens. In light of recent natural disasters, with reported damages and evacuations, hospital facilities have strict laws to enforce seismic upgrades in order to remain operational. Senate Bill 1953 was introduced as part of the Alfred E. Alquist Hospital Facilities Seismic Safety Act of 1983 in which California hospitals were assigned a structural performance category [32]. This ranking correlates to a timeline in which the facility must perform a seismic retrofit in order to ensure operation after an earthquake [33]. Legislation such as this ensures that not only structures, but the community, are prepared should a seismic event occur in the region.

While the focus here is remaining operational after a natural disaster, it is important to note that as stated in the design prompt in **Section 2**, the COVID-19 pandemic was a large motivator for this year's competition. As such, if these laws were not in place, the capacities of hospitals could have been even more in demand, as construction could have halted the use of the facilities from remaining operational.

8.2 GLOBAL IMPACT

While this report focused on the redesign and retrofit of a hospital structure in Seattle, WA, a similar approach can be applied to any structure in an area of high seismic activity. It is important to note that while earthquake engineering policy and practices have grown in the United States, it is the 7th most prone country to earthquakes, behind some developing countries [34]. Natural disasters are becoming more alarming and can devastate communities in which they occur. According to the World Health Organization, "more than 125 million people were affected by earthquakes from 1998-2017" [35]. This global number includes those who were made homeless, displaced, or evacuated during the emergency. All of these circumstances stem from lack of proper seismic preparedness of the structures, including healthcare facilities in their community. These essential facilities are needed to treat those injured as a result of an earthquake. Following the magnitude 8.8 Chile Earthquake of 2010, the Chilean Ministry of Health reported to EERI that "four hospitals became uninhabitable, twelve had greater than 75% loss of function, eight were operating only partially after the main shock, and 62% needed repairs or replacement" [36]. The lack of healthcare facilities available make a vast difference in times of need and can ultimately be a matter of life or death. The alarming amount of people worldwide that are

impacted by earthquakes each year translates to the need for more seismic upgrades to be performed on a more global scale.

8.3 CULTURAL IMPACT

The cultural vibrancy of many cities, including Seattle, have historic roots that tie back to the infrastructure in the region. Historical buildings are an important part of the cultural heritage in both their architecture and engineering. Their conservation over the centuries is vital to pass on to future generations. With seismic retrofits and redesigns, this cultural aspect of structures is able to be maintained and preserved. Seattle alone has eight historic districts with over 400 preserved structures [37]. With the hospital structure being in close proximity to other historic structures, it is important to define residual displacements and how these can create a fall-zone hazard for surrounding structures. Buildings subjected to strong earthquake motions may be left in a displaced condition which is undesirable as it presents problems during repair and reconstruction [38]. Most notably, after the 2011 magnitude 6.3 Canterbury earthquake in Christchurch, New Zealand, among the severely damaged structures was the 26-story Grand Chancellor Hotel which was permanently leaning, and a two-block radius of surrounding structures were cordoned off [39]. This led to the evacuation of structures that could have otherwise been occupied. This concern arises with taller structures being built in historic neighborhoods, where a seismic event could result in a collapse of the new structure, which then in turn could wipe out historic structures. Ensuring these buildings and landmarks are safe for the future, helps ensure the culture of the city is there for years to come.

8.4 SOCIAL IMPACT

The aftermath of a seismic event forces a loss of community in the city, as people are displaced and forced to flee the region or even the country. The destruction and loss of life that so often follows an earthquake forces a shift in the society that preceded. Due to the immense loss, change, and trauma, there is a great toll on the mental health of survivors. One study found that one-third of survivors suffered from a post-disaster diagnosis, followed by 16% having major depression, and 9% suffering from alcohol abuse [40]. The rise of a mental health crisis following an earthquake has a major impact on the social well-being of the community.

Cities have recently been introducing community resilience programs ensuring the ability to recognize risk, adapt changing conditions, relieve social stresses, and recover rapidly from hazard events [41]. Communities have become more earthquake-resilient by implementing credible plans that contribute to long term community goals while protecting the overall well-being of the citizens after a disaster. Policies, such as these, ensure community resiliency that will lead to a new and better normal once recovered. The redesign and retrofit of this Seattle hospital, or any hospital for that matter, will deepen the resiliency of the community and prepare them for whatever is to come.

8.5 ENVIRONMENTAL IMPACT

The building sector contributes greatly to global warming with the emission of carbon dioxide and methane causing pollution and waste. With a shift towards a carbon-neutral society, there has been a growth in retrofits and remodels of older structures, often referred to as adaptive reuse. During design of this nature, environmental considerations that can bring a building up to the LEED standards can be incorporated. Buildings are first assessed in terms of energy redesign then analyzed for need of seismic retrofit [42]. Despite all the advancements in green construction, retrofitting an existing building is a more sustainable option than tearing down and rebuilding. Similarly, ensuring buildings are seismically resilient before an earthquake even happens, is a sustainable option that takes precaution into account [43]. With the already alarming concerns over global warming in the building industry, by retrofitting and remodeling more existing structures, a shift in the environmental impact of the industry will be recognized.

8.6 ECONOMIC IMPACT

While the upfront cost of a retrofit may be significant, it is nothing of the economic toll that follows a natural disaster. Taking preventative measures serves as a way to mitigate potentially catastrophic effects by not only preparing the structure to perform in an earthquake, but also ensuring the safety of any occupants. In a study from the University of Architecture and Urbanism in Bucharest, Romania, substantial savings are to be expected when compared to repair costs after a variety of earthquakes. The researchers found that the cost for repair, depending on the ground motion, can be anywhere from three to eight times more expensive than the preventative measure [44]. Not only are retrofits more cost effective than earthquake damage repairs, they also can increase the life of an existing structure, thus minimizing the need for demolition and construction of a new buildings. With this option becoming more attractive, it is likely more structures will remain operational as they have been updated to collapse prevention standards.

9 PERSONAL REFLECTION

I have been involved with the Cal Poly EERI Student Chapter since my freshman year. At that time, I could not fathom all that goes into ensuring a structure is stable, as well as prepared for a seismic event. Through my involvement in the EERI Seismic Design Competition these past four years, I have gained an immense amount of knowledge in the field of earthquake engineering. These experiences coupled with my coursework in Architectural Engineering, I feel extremely prepared to enter industry upon graduation.

I have learned many skills that I will carry with me from my time with EERI, but more specifically from this year's competition. As Team Captain, I was tasked with leading a team of eight board members as well as other club members to compete in an entirely virtual competition comprised of four lengthy and technically rigorous deliverables along with a poster and oral presentations. Balancing all these tasks with the coursework that comes with ARCE design labs was a challenge for me and helped me strengthen my time management skills. Any time outside of class, homework, and projects was spent on the competition. While some EERI SDC competition tasks were delegated to underclassmen, there was only so much they were prepared to assist with given their completed coursework, enforcing the importance of delegation when needed.

Completion of this report enabled me to conduct further design and analysis activities that were limited during the brief timeframe of the competition. Throughout this process, I leaned on my professors to assist with design and technical aspects of the competition, from help with ETABS 19 modeling to how to read a P-S Suspension Log. Meetings with various professors over Zoom provided the necessary background that ensured the success of our team. The use of structural design codes was also a great tool, especially during the Geotechnical Deliverable, where many assigned tasks came straight out of ASCE 7-16 [1]. The ARCE curriculum greatly prepared other senior team members and I to already be comfortable with the code and much of what we were being asked to do during the competition had been outlined in our design courses in parallel with the code. Lastly, when professors and the code did not have the answers we were seeking, I turned to the internet and reliable websites and technical papers that specified niche topics I wanted to gain clarity on.

The virtual competition setting highlighted our team's strengths of communication and collaboration. Since this year's competition deliverables and format greatly differed from those of the past it was of utmost importance to ensure communication between all student team members. This included ensuring whenever team members were working on the deliverables, they were partnered with someone in a Zoom meeting. This not only allowed for collaboration, but communication on what is getting done and what still needs work on. Outside of these Zoom calls, messaging was frequent between team members to check in on assigned tasks.

Overall, keeping track of all the team's tasks proved difficult. But through all the hardships and Zoom calls, I was still able to gain all the benefits that this competition has to offer. The overall design process of a base structure in addition to a seismic retrofit allowed me to gain exposure in areas of study including geotechnical engineering, architecture, construction processes, earthquake

engineering, cost analysis, and structural engineering. Topics learned in these areas will help ensure I become a well-rounded structural engineer. The research, design, and analysis methods that were used throughout the competition have also strengthened my understanding of modeling tools. As I enter the field of structural engineering, I plan to relay the importance of earthquake engineering and how it can be applied to any structure, whether it be existing or new design.

10 CONCLUSION

With direction from the mayor of Seattle, WA an addition to a hospital structure in the Belltown Neighborhood was proposed to increase patient capacity in response to demands from COVID-19.

This report summarized seismic evaluations conducted for this structural upgrade. Once subsurface geotechnical and seismicity conditions were assessed, ground motions were scaled to best represent the seismic hazard. Then scaled earthquake ground motions were input into the ETABS model for the original 10-story structure developed from the provided drawings.

Different design options for the vertical structural addition were considered. Once a final brace layout for the extension was selected, with architectural considerations in mind, it was assessed based on interstory drift and member forces. At that stage, the structure's design was insufficient, and a retrofit of the entire hospital was undertaken in which the bracing layout and member sizes were modified. Further time history analyses of the retrofitted hospital proved that interstory drift and member demands were now acceptable. Final drawings, including plans and elevations, were then produced in Revit to document the design.

As a package, these deliverables were able to combine research, design, and analysis from multiple disciplines in order to achieve a successful redesign and retrofit of a Seattle hospital. Overall, the participation in the 2021 EERI Seismic Design Competition allowed students, including the author of this report who served as the team captain, to begin to recognize the importance of earthquake engineering from the standpoint of a practitioner and how it aligns with the coursework taught in the Architectural Engineering Department at the Cal Poly - San Luis Obispo.

11 REFERENCES

[1] Minimum Design Loads and Associated Criteria for Buildings and Other Structures. American Society of Civil Engineers, 2017. doi: 10.1061/9780784414248

[2] Seismic Evaluation and Retrofit of Existing Buildings. American Society of Civil Engineers, 2017. doi: 10.1061/9780784414859

[3] Supplement: Design Values for Wood Construction. National Design Specifications, 2018. ISBN: 978-1-940383-43-9

[4] J. Johansson, "Which Soils Are Liquefaction Susceptible?," *Washington.edu*, 2000. https://depts.washington.edu/liquefy/html/how/susceptible.html.

[5] J. D. Bray and R. B. Sancio, "Assessment of the Liquefaction Susceptibility of Fine-Grained Soils," *Journal of Geotechnical and Geoenvironmental Engineering*, vol. 132, no. 9, pp. 1165–1177, Sep. 2006, doi: 10.1061/(asce)1090-0241(2006)132:9(1165).

[6] R. W. Boulanger and I. M. Idriss, "Liquefaction Susceptibility Criteria for Silts and Clays," *Journal of Geotechnical and Geoenvironmental Engineering*, vol. 132, no. 11, pp. 1413–1426, Nov. 2006, doi: 10.1061/(asce)1090-0241(2006)132:11(1413).

[7] The Constructor. (n.d.). *Ground Improvement Techniques for Stabilization of Soil for Various Purposes*. The Constructor: Building Ideas. https://theconstructor.org/geotechnical/ground-improvement-techniques-soil-stabilization/1836/

[8] "Seattle Office of Emergency Management Seattle Hazard Identification and Vulnerability Analysis Earthquakes Key Points." Accessed: Jan. 31, 2021. [Online]. Available: https://www.seattle.gov/Documents/Departments/Emergency/PlansOEM/SHIVA/2014-04-23_Earthquakes(0).pdf.

[9] J. Czajkowski and J. Bowman, "Faults and Earthquakes in Washington State," *Faults and Earthquakes in Washington State*. https://www.dnr.wa.gov/publications/ger_ofr2014-05_fault_earthquake_map.pdf

[10] Science Education Research Center. (2019). *Case Study: Analyzing Tectonic Plate Motion with GPS Data*. Carleton College. https://serc.carleton.edu/eet/platemotion/case_study.html

[11] Bray, J. D., Sancio, R. B., Kammerer, A. M., Merry, S., Rodriguez-Marek, A., Khazai, B., Chang, S., Bastani, A., Collins, B., Hausler, E., Dreger, D., Perkins, W. J., & Nykamp, M. (2001, March). *Some Observations of Geotechnical Aspects of the February 28, 2001, Nisqually Earthquake in Olympia, South Seattle, and Tacoma, Washington*. Geotechnical Extreme Events Reconnaissance. http://www.geerassociation.org/administrator/components/com_geer_reports/geerfiles/Nisqually_2001/indexa.html

[12] King, A., & Campbell, K. (2021, February 25). *Two decades later: What's changed since the Nisqually earthquake?* Https://Www.Kuow.Org/Stories/Two-Decades-Later-What-s-Changed-since-the-Nisqually-Earthquake. https://www.kuow.org/stories/two-decades-later-what-s-changed-since-the-nisqually-earthquake

[13] Dunagan, C. (2006, February 28). Nisqually Earthquake Still Heeds Warnings for County. *Kitsap Sun*. http://archive.kitsapsun.com/news/local/editors-choice-nisqually-earthquake-still-heeds-warnings-for-county-ep-423415882-359485861.html

[14] *Unified Hazard Tool*. (n.d.). United States Geological Survey. https://earthquake.usgs.gov/hazards/interactive/
[15] *ATC Hazards by Location*. (n.d.). Applied Technology Council. https://hazards.atcouncil.org/#/seismic?lat=47.6163&lng=-122.3534&address=
[16] *PEER Ground Motion Database*. (2014). Pacific Earthquake Engineering Research Center. https://ngawest2.berkeley.edu/
[17] *ETABS*. (2018). [Software]. Computers & Structures, Inc. https://www.csiamerica.com/products/etabs
[18] Cannon, Jr, D. D. & University of Tennessee, Knoxville. (1984). *Determination of Column Fixity at Column Bases*. American Institute of Steel Construction. https://www.aisc.org/globalassets/aisc/research-library/determination-of-column-fixity-at-column-bases.pdf
[19] *What is A36 Steel?* (2015, September 25). SteelFront | Steel Parts and Accessories. https://steelfront.com/what-is-a36-steel/
[20] Xiang, Y., Naeim, F., & Zareian, F. (2020). Evaluation of natural periods and modal damping ratios for seismic design of building structures. *Earthquake Spectra*. https://doi.org/10.1177/8755293019900776
[21] Miranda, E., & Cruz, C. (2020, October). *Damping Ratios of the First Mode for the Seismic Analysis of Buildings*. American Society of Civil Engineers. https://ascelibrary.org/doi/10.1061/%28ASCE%29ST.1943-541X.0002873
[22] *Floor Diaphragms*. Structural Engineering Forum of India. https://www.sefindia.org/forum/files/floor_diaphragms_353.pdf
[23] Chopra, A. K. (2011). *Dynamics of Structures (4th Edition) (Prentice-hall International Series in Civil Engineering and Engineering Mechanics)* (4th ed.). Pearson.
[24] MATLAB and Statistics Toolbox Release R2020b, The MathWorks, Inc., Natick, Massachusetts, United States.
[25] Paal, S. G., Vick, S., & Kopsida, M. (2020). Use Cases for Architects and Engineers. *Infrastructure Computer Vision*, 203–266. https://doi.org/10.1016/b978-0-12-815503-5.00005-x
[26] Choi, G., Ho, G., Joseph, L., Mathias, N., & C. (2017). *Outrigger Design for High-Rise Buildings*. Amsterdam University Press.
[27] *US Bank Tower, Milwaukee*. (n.d.). [Photograph]. https://statetrunktour.com/poi/us-bank-tower-milwaukee/
[28] *Touring NYC's 425 Park Avenue Transformation*. (2018, October 12). Modern Steel Construction. https://www.aisc.org/modernsteel/news/2018/october/steel-shots-touring-nycs-425-park-avenue-transformation/
[29] *425 Park Avenue*. (2020, November 27). Adamson and AAI. https://www.adamson-associates.com/project/425-park-avenue/
[30] *Revit*. (2020). [Software]. Autodesk. https://www.autodesk.com/products/revit/overview
[31] *LEED rating system*. (2021). U.S. Green Building Council. https://www.usgbc.org/leed
[32] *Program Overview*. (2019, September 13). Office of Statewide Health Planning and Development. https://oshpd.ca.gov/construction-finance/seismic-compliance-and-safety/program-overview/
[33] *Seismic Compliance and Safety*. (2021, March 12). Office of Statewide Health Planning and Development. https://oshpd.ca.gov/construction-finance/seismic-compliance-and-safety/

[34] Nag, O. S. (2019, April 11). *The World's 10 Most Earthquake Prone Countries*. WorldAtlas. https://www.worldatlas.com/articles/the-world-s-10-most-earthquake-prone-countries.html
[35] *Earthquakes*. (2019, November 8). World Heath Organization. https://www.who.int/health-topics/earthquakes#tab=tab_1
[36] *Learning from Earthquakes: The Mw 8.8 Chile Earthquake of February 27, 2010*. (2010, June). EERI Special Earthquake Report.
[37] *Historic Preservation - Neighborhoods*. (2020, March 3). Seattle Department of Neighborhoods. https://www.seattle.gov/neighborhoods/programs-and-services/historic-preservation#:%7E:text=Seattle's%20eight%20historic%20districts%20and,importance%20are%20valuable%20cultural%20assets
[38] Kawashima, K., MacRae, G. A., Hoshikuma, J., & Nagaya, K. (1998). Residual Displacement Response Spectrum. In Journal of Structural Engineering (Vol. 124, Issue 5, pp. 523–530). American Society of Civil Engineers (ASCE). https://doi.org/10.1061/(asce)0733-9445(1998)124:5(523)
[39] Post, Nadine M. "Christchurch Cordons off Area around Damaged 26-Story Hotel." *Engineering NewsRecord RSS*, Engineering News-Record, 29 Oct. 2015, https://www.enr.com/articles/3451-christchurch-cordons-off-area-around-damaged-26-story-hotel.
[40] Lin, R., II. (2019, December 13). *After a big earthquake, a public mental health crisis will follow*. Los Angeles Times. https://www.latimes.com/california/story/2019-12-12/how-the-next-big-earthquake-will-worsen-mental-health
[41] EERI Board of Directors. (n.d.). *Creating Earthquake-Resilient Communities*. Earthquake Engineering Research Institute. Retrieved July 12, 2021, from https://www.eeri.org/advocacy-and-public-policy/creating-earthquake-resilient-communities/
[42] Belleri, A., & Marini, A. (2016). Does seismic risk affect the environmental impact of existing buildings? *Energy and Buildings*, *110*, 149–158. https://doi.org/10.1016/j.enbuild.2015.10.048
[43] S. (2021, November 24). *US Resiliency Council - Building Community Resilience*. US Resiliency Council. https://www.usrc.org/
[44] Bostenaru Dan, M. (2018). Decision Making Based on Benefit-Costs Analysis: Costs of Preventive Retrofit versus Costs of Repair after Earthquake Hazards. *Sustainability*, *10*(5), 1–26. https://doi.org/10.3390/su10051537

12 APPENDIX

Appendix 4.1.3

4.1.3 Shear Wave Velocity Calculation [1]				
Depth	S-wave Velocity, Vsi	di Calculation	Layer Thickness, di	di / Vsi
ft	ft / sec		ft	
7.9	690	7.9 - 0	7.9	0.0114
9.8	973	13.1 - 7.9	5.2	0.0053
13.1	428	16.4 - 9.8	6.6	0.0154
16.4	389	19.7 - 13.1	6.6	0.0170
19.7	520	23.0 - 16.4	6.6	0.0127
23.0	541	16.2 - 19.7	6.5	0.0120
26.2	402	29.5 - 23.0	6.5	0.0162
29.5	479	32.8 - 26.2	6.6	0.0138
32.8	364	36.1 - 29.5	6.6	0.0181
36.1	503	39.4 - 32.8	6.6	0.0131
39.4	663	42.6 - 36.1	6.5	0.0098
42.6	663	46.2 - 39.4	6.8	0.0103
46.2	925	49.2 - 42.6	6.6	0.0071
49.2	499	52.5 - 46.2	6.3	0.0126
52.5	792	55.8 - 49.2	6.6	0.0083
55.8	517	59.0 - 52.5	6.5	0.0126
59.0	559	62.3 - 55.8	6.5	0.0116
62.3	800	65.6 - 59.0	6.6	0.0082
65.6	669	68.9 - 62.3	6.6	0.0099
68.9	362	72.5 - 65.6	6.9	0.0191
72.5	554	75.4 - 68.9	6.5	0.0117
75.4	876	78.7 - 72.5	6.2	0.0071
78.7	772	82.0 - 75.4	6.6	0.0085
82.0	697	85.3 - 78.7	6.6	0.0095
85.3	671	88.6 - 82.0	6.6	0.0098
88.6	800	85.3 - 91.8	6.5	0.0081
91.8	426	95.1 - 88.6	6.5	0.0153
95.1	620	98.4 - 91.8	6.6	0.0106
98.4	782	101.7 - 95.1	6.6	0.0084
101.7	790	101.7 - 98.4	3.3	0.0042

Σ di	Σ di / Vsi
193.6	0.3379
Vs, avg (ft / sec) =	**573**

20.4.1 $\bar{v}_s$, Average Shear Wave Velocity. $\bar{v}_s$ shall be determined in accordance with the following formula:

$$\bar{v}_s = \frac{\sum_{i=1}^{n} d_i}{\sum_{i=1}^{n} \frac{d_i}{v_{si}}} \qquad (20.4\text{-}1)$$

where

d_i = the thickness of any layer between 0 and 100 ft (30 m);
v_{si} = the shear wave velocity in ft/s (m/s); and
$\sum_{i=1}^{n} d_i$ = 100 ft (30 m).

Appendix 4.2.4.1

4.2.4.1 Design Criteria for Response Spectrum		
Site Class	D	ASCE 7-16, 20.3.1 [1] & *Supplement 4-3*
Seismic Design Category	D	ASCE 7-16, Section 11.6 [1]
Risk Category	IV	ASCE 7-16, Table 1.5-1 [1]
S_a (T=1.0 second)	0.29 g	ASCE 7-16, Equation 11.4-6 [1]
S_a (T=2.0 seconds)	0.59 g	ASCE 7-16, Equation 11.4-6 [1]
S_s	1.39	ATC Hazard Tool [14]
S_1	0.49	ATC Hazard Tool [14]
S_{MS}	1.39	ATC Hazard Tool [14]
S_{DS}	0.93	ATC Hazard Tool [14]
F_a	1.00	ASCE 7-16, Table 1.4-1 [1]
F_v	1.82	ASCE 7-16, Table 1.4-2 [1]
S_{M1}	0.88	ASCE 7-16, Equation 11.4-2 [1]
S_{D1}	0.59	ASCE 7-16, Equation 11.4-4 [1]
T_0	0.13 s	ASCE 7-16, Section 11.4.6 [1]
T_S	0.63 s	ASCE 7-16, Section 11.4.6 [1]
T_L	6.00 s	ATC Hazard Tool [14]

Appendix 5.2.3.2

REFERENCE	CALCULATIONS FOR CAPACITY OF BALSA WOOD MEMBERS
NDS 2018 SECTION	**BENDING CAPACITY** $F_b' = F_b\,(C_D)(C_M)(C_t)(C_L)(C_F)(C_{fu})(C_i)(C_r)$ [ASD FACTORS]
2.3.2	$C_D = 1.6$ B/C EARTHQUAKE LOADING
4.1.4 & 5.1.4	$C_M = 1.0$ ASSUMING MEMBER IS UNDER NORMAL CONDITIONS W/ MC ≥ 19%
2.3.3	$C_t = 1.0$ MEMBER IN CONDITIONED SPACE W/ NO CONCERN FOR EXTREME TEMPERATURES
3.3.3	$C_L = 1.0$ B/C $b = 0.12'' \geq d = 0.12''$ ✓
4.3.6	$C_F = 1.5$ B/C 2X WIDTH AND THICKNESS
4.3.7 & 5.3.7	$C_{fu} = 1.0$ N/A
4.3.8	$C_i = 1.0$ B/C NOT EXPOSED TO EXTERNAL CONDITIONS
4.3.9	$C_r = 1.0$ B/C BEAMS ONLY ON MAJOR GRIDLINES AND IN SCALED UP MODEL "JOISTS" WOULD BE SPACED FURTHER THAN 24" O.C.
	$F_b' = 2000\ psi\,(1.6)(1.0)(1.0)(1.0)(1.5)(1.0)(1.0)(1.0)$ $F_b' = 4800\ psi$
NDS 2018 SECTION	**SHEAR CAPACITY** $F_v' = F_v\,(C_D)(C_M)(C_t)(C_i)$ [ASD FACTORS]
2.3.2	$C_D = 1.6$ B/C EARTHQUAKE LOADING
4.1.4 & 5.1.4	$C_M = 1.0$ ASSUMING MEMBER IS UNDER NORMAL CONDITIONS W/ MC ≥ 19%
2.3.3	$C_t = 1.0$ MEMBER IN CONDITIONED SPACE W/ NO CONCERN FOR EXTREME TEMPERATURES
4.3.8	$C_i = 1.0$ B/C NOT EXPOSED TO EXTERNAL CONDITIONS
	$F_v' = 200\ psi\,(1.6)(1.0)(1.0)(1.0)$ $F_v' = 320\ psi$
NDS 2018 SECTION	**TENSION CAPACITY** $F_t' = F_t\,(C_D)(C_M)(C_t)(C_F)(C_i)$ [ASD FACTORS]
2.3.2	$C_D = 1.6$ B/C EARTHQUAKE LOADING
4.1.4 & 5.1.4	$C_M = 1.0$ ASSUMING MEMBER IS UNDER NORMAL CONDITIONS W/ MC ≥ 19%
2.3.3	$C_t = 1.0$ MEMBER IN CONDITIONED SPACE W/ NO CONCERN FOR EXTREME TEMPERATURES
4.3.6	$C_F = 1.5$ B/C 2X WIDTH AND THICKNESS
4.3.8	$C_i = 1.0$ B/C NOT EXPOSED TO EXTERNAL CONDITIONS
	$F_t' = 1200\ psi\,(1.6)(1.0)(1.0)(1.5)(1.0)$ $F_t' = 2880\ psi$
NDS 2018 SECTION	**COMPRESSION CAPACITY** $F_c' = F_c\,(C_D)(C_M)(C_t)(C_F)(C_i)(C_p)$ [ASD FACTORS]
2.3.2	$C_D = 1.6$ B/C EARTHQUAKE LOADING
4.1.4 & 5.1.4	$C_M = 1.0$ ASSUMING MEMBER IS UNDER NORMAL CONDITIONS W/ MC ≥ 19%
2.3.3	$C_t = 1.0$ MEMBER IN CONDITIONED SPACE W/ NO CONCERN FOR EXTREME TEMPERATURES
4.3.6	$C_F = 1.5$ B/C 2X WIDTH AND THICKNESS
4.3.8	$C_i = 1.0$ B/C NOT EXPOSED TO EXTERNAL CONDITIONS
3.7.1	$C_p = \frac{1+(F_{cE}/F_c^*)}{2c} - \sqrt{\left[\frac{1+(F_{cE}/F_c^*)}{2c}\right]^2 - \frac{F_{cE}/F_c^*}{c}}$, $c = 0.8$ SAWN LUMBER
	$F_c = 900\ psi$ $F_c^* = 900\ psi\,(1.6)(1.0)(1.0)(1.5)(1.0) = 2160\ psi$ $(l_e/d)_{BM} = 2''/0.12'' = 16.7$ $(l_e/d)_{COL} = 3''/0.2'' = 15$ → BM WORST CASE
	$F_{cE} = \frac{0.822E'_{min}}{(l_e/d)^2} = \frac{0.822\,(350{,}000\ psi)(1.0)}{(2''/0.12'')^2} = 1035\ psi$
	$C_p = \frac{1+(1035/2160)}{2(0.8)} - \sqrt{\left(\frac{1+1035/2160}{2(0.8)}\right)^2 - \frac{1035/2160}{1.6}} = 0.42$
GIVEN	$F_c' = F_c^*(C_p) = 2160\ psi\,(0.42)$ $F_c' = 905\ psi$

Appendix 7.2.1

Approximation of Construction Schedule and Sequence		
Work Days	**Activity**	**Timeline**
	Pre-Construction	
45 +/-	Design Addition	
20 +/-	Produce Construction Documents	(Start During Last Week of Design)
30+	Obtain Financing	(Start After Design Documents)
90+	Obtain Permits	(Start After Design Documents)
1	Sign Contract	(Day After Permits are Obtained)
	Start Construction	
14	Visit Existing Site to Confirm Drawings	(Start After Contract is Signed)
7	Test Equipment for Noise and Vibrations	(Start Two Days After Site Visits)
7	Complete Parking Study for Placement of Construction Facilities	(Start Two Days After Testing)
4	Meet with Hospital Staff for Typical Daily Occupancy	(Start After Parking Testing is Completed)
11	Establish Emergency Protocols	(Start After Meeting with Staff)
11	Layout Building	(Start After Emergency Protocols)
4	Install Backup Generators	(Start After Layout Building)
8	Rough Framing: 1st Floor of Addition	(Start After Generators are Installed)
7	Rough Plumbing	(Start After Rough Framing Completed)
7	Rough Mechanical	(Start After Rough Plumbing Completed)
1	INSPECTION: Framing, Plumbing, HVAC	(Day After Rough Mechanical Completed)
90	Rough Framing: Addition	(Start After Inspection)
1	INSPECTION: Structural Sheathing	(Day After Rough Framing Completed)
14	Roofing	(Start Last Week of Rough Framing)
11	Gutters	(Start After Roofing Completed)
1	Haul Trash	(Start Last Day of Roofing)
17	Windows	(Start After Roofing Completed)
17	Rough Plumbing	(Start Same Day of Structural Sheathing Inspection)
17	Rough Mechanical	(Start After First Week of Plumbing)
17	Rough Electrical	(Start After First Week of Mechanical)
8	Rough Alarm Wiring	(Start After First Week of Electrical)
28	Exterior Finishes	(Start on Last Day of Rough Wiring)
1	INSPECTION: Structural, Plumbing, Mechanical, Electrical	(Day After Exterior Finishes Complete)
14	Insulation	(Start After Second Week of Exterior Finishes)
1	INSPECTION: Insulation	(Day After Insulation Completed)
31	Hang Drywall	(Start After Insulation Inspection)
1	INSPECTION: Drywall Nailing	(Day After Inspection)
1	Haul Trash	(Same Day as Drywall Inspection)
25	Drywall Finish	(Start After Drywall Inspection)
14	Finish Carpentry: Hang doors	(Start After Finish Drywall)
14	Finish Carpentry: Trim (windows, doors, baseboard)	(Start After Hang Door)
14	Finish Carpentry: Stairs	(Start After Finish Drywall)
21	Paint/Stain: rails, drywall, gutters, siding	(Start After Stairs)
6	Initial Finish Plumbing	(Start After Finish Carpentry Completed)
11	Finish Mechanical	(Start After Finish Plumbing)
17	Finish Electrical	(Start After Finish Mechanical)
4	Finish Security Alarm	(Start After Finish Electrical)
10	Finish Hardware	(Start After Finish Security Alarm)
10	Final Finish Carpentry	(Start After Finish Hardware)
10	Final Finish Plumbing	(Start After Final Finish Carpentry)
21	Flooring	(Start After Final Finish Plumbing)
6	Final Cleanup	(Start After Flooring Completed)
3	Miscellaneous Electrical	(Start After Final Cleanup)
7	Final Paint (Touch Up)	(Start After Flooring Completed)
3	Haul Trash	(Start After Final Paint Completed)
1	Final Inspection / Certification of Occupancy	(Start on Last Day of Haul Trash)
1	FINAL INSPECTION	(Day After CO)
750	Total Days (if consecutive work)	